Author's personal copy

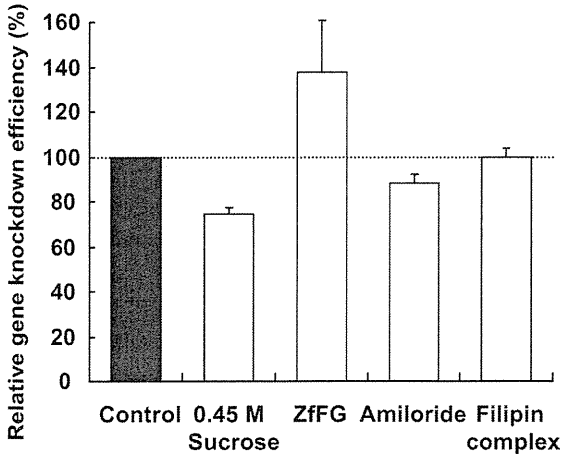

Fig. 6. The major uptake route contributing to the gene knockdown effect of vor-LTsiR. Data represent the mean ± S.D. of three independent experiments performed in triplicate. Cells were transfected with vor-LTsiR in the absence (control) or in the presence of sucrose, ZfFG, amiloride or filipin complex. GFP fluorescence was measured at 22 h after transfection by flow cytometry.

only around 36% of the siRNA attached to a relative lipoplex size (Fig. 2). Given the same lipid concentration, a smaller lipoplex size would equate to a larger total surface area. A larger total surface area for lipoplex can promote extensive interactions with target cells. Hence, the higher gene knockdown efficiency induced by vor-LTsiR at a relatively lower siRNA dose (Fig. 1) might be due to the efficient delivery of siRNA into the cells as a result of the enhanced interaction of the lipoplex with the cells. This assumption is strongly supported by the results of qualitative and quantitative analysis, as described in Figs. 3 and 4.

From the mechanism of RNAi, the intracellular presence of siRNA molecules complementary to the target mRNA is of crucial importance for inducing gene knockdown (Behlke, 2006; Li et al., 2006). Therefore, it is essential that the siRNA lipoplex is taken up intact by the cells, and that the lipoplex efficiently releases the siRNA molecule into the cytoplasm (Khalil et al., 2006a). As shown in Fig. 3, in the vor-LTsiR, LT (red) was extensively co-localized with siRNA (green), indicating that the lipoplex associated with siRNA was efficiently internalized in the cells. In the spo-LTsiR, however, the LT (red) was less co-localized with siRNA (green), indicating either that the lipoplex were associated with fewer siRNA or that empty LT were internalized. In addition, the result of semi-quantitative evaluation (Fig. 4) indicated that vor-LTsiR improved 3-fold the amount of siRNA internalized in the cells compared with spo-LTsiR, although there was no significant difference in the total amount of siRNA and LT that interacted with the cells between both formulations. Accordingly, the superior gene knockdown efficacy of vor-LTsiR observed in Fig. 1 may be explained by the following scenario: the smaller sized (≤200 nm) vor-LTsiR contained a large amount of siRNA (Fig. 2A) and were extensively taken up by the targeted cells (Fig. 4 left). However, the smaller sized (≤200 nm) spo-LTsiR contained fewer siRNA (Fig. 2B) that were taken up by the cells and the remaining spo-LTsiR (≥200 nm) simply associated with the cell surface, which limited or delayed their internalization. Several studies have demonstrated that the uptake of viral particles (Matlin et al., 1982), polyplexes (Godbey et al., 1999), and beads (Rejman et al., 2004) by cells is delayed in a size-dependent manner.

Particle size determines the pathway of cellular entry, and therefore, also determines the kinetics of internalization and the intracellular trafficking of the particles (Rejman et al., 2004; Gratton et al., 2008). There is convincing evidence that endocytosis represents the major pathway of entry into cells for particles <1 μm in size (Rejman et al., 2004; Spagnou et al., 2004; Khalil et al., 2006a; Hoekstra et al., 2007; Gratton et al., 2008). These pathways include phagocytosis, clathrin-dependent endocytosis and clathrin-independent endocytosis, the latter including macropinocytosis and internalization via caveolae (Rejman et al., 2004; Khalil et al., 2006a; Sahay et al., 2010). In the present study, three pathways were found in the uptake of both lipoplexes by cells. As shown in Fig. 5, the internalization of vor-LTsiR was mainly via clathrin-mediated endocytosis while macropinocytosis and cell fusion were secondary routes. On the contrary, the internalization of spo-LTsiR was mainly through membrane fusion while macropinocytosis and clathrin-mediated endocytosis were secondary routes. At present, the majority of reports suggest that positively charged nanomaterials predominantly internalize through clathrin-mediated endocytosis with some fraction utilizing macropinocytosis (Sahay et al., 2010). Our current results are consistent with the previous reports.

Clathrin-mediated endocytosis and macropinocytosis have been suggested as the major routes of cellular entry for lipoplexes containing nucleic acids such as pDNA and siRNA (Thomsen et al., 2002; Zuhorn et al., 2002; Zhang et al., 2003; Nakase et al., 2004; Spagnou et al., 2004; Wadia et al., 2004; Kaplan et al., 2005; Rejman et al., 2005; Khalil et al., 2006a; Sahay et al., 2010). The present study also clearly showed that both routes are major inducements of the vor-LTsiR-mediated gene silencing effect (Fig. 6). Under normal conditions, the formation of clathrin-coated pits is very rapid (within 28 s), with the entire population of coated pits being turned over approximately every 6 min, making this structure highly mobile (Kawakami et al., 2002). Particles of 50 and 100 nm in size are internalized in a relatively rapid process by this pathway (Rejman et al., 2004). Hence, it is assumed that the lipoplex of vor-LTsiR (≤200 nm), which contains 80% siRNA, are quickly and extensively internalized (Figs. 3 and 4), resulting in an efficient gene-knockdown effect (Fig. 1). Macropinocytosis is known as an efficient route for the nonselective endocytosis of solute macromolecules and provides some advantageous aspects on siRNA-based gene-knockdown such as the avoidance of lysosomal degradation and an easing of the escape from macropinosomes (Khalil et al., 2006a). However, in the present study, it appears that macropinocytosis only partly contributes to vor-LTsiR-mediated gene silencing.

Cationic liposome, including lipoplex, is known to interact and fuse with cell membranes (Leventis and Silvius, 1990). Fusion was one of the major cellular entry routes for spo-LTsiR, which agrees with previous reports (Fig. 5). Size is known to be one of the most important factors affecting the dynamics of vesicle sedimentation onto the cells (Faneca et al., 2004). In the present study, lipoplexes formed spontaneously in Opti-MEM, the transfection medium, and presented a wider size distribution due to the relatively uncontrolled process of association between siRNA and LT. Accordingly, in spo-LTsiR, approximately 64% of siRNA preferentially attached to lipoplexes larger than 200 nm in size (Fig. 2). Assuming that spo-LTsiR (≥200 nm) is taken up only to a limited extent by macropinocytosis, the remaining lipoplexes bound to the cell surface are assumed to be held at the cell surface for a relatively longer period. Such a long period on the cell surface might lead to the progressive dilution of the lipoplexes as the cell divide (Leung and Whittaker, 2005). In addition, extensive leakage of contents from phosphatidylethanolamine-based liposomes is known to occur during fusion (Brown and Silvius, 1989). This may expose the siRNA associated with, or released from, the spo-LTsiR to potential enzymatic or physical degradation before it can reach the cytoplasm (Spagnou et al., 2004). Consequently, spo-LTsiR might have shown a lower gene knockdown effect in the present study (Fig. 1).

Author's personal copy

5. Conclusion

The present study showed that the preparation procedure for siRNA-lipoplex remarkably affects the *in vitro* gene-knockdown efficiency of siRNA. Smaller (≤200 nm) and relatively homogeneous lipoplexes containing a large amount of siRNA (80% of dose), produced by agitation (vortex-mixing) during the preparation, allowed for the efficient cellular interaction of lipoplex and a shift in their entry pathway from fusion to clathrin-mediated endocytosis, resulting in an increased amount of siRNA internalized in cells, and thereby, an enhanced gene-knockdown efficacy. A proper siRNA-lipoplex preparation procedure was strongly related to both the efficiency of cellular uptake and the gene-knockdown efficiency of siRNA. The results of the present study may have implications for designing a more efficient and successful siRNA delivery system.

Acknowledgements

The authors thank Dr. James L. McDonald for his helpful advice in developing the English manuscript. This work was supported in part by the Health and Labour Sciences Research Grants for Research on Advanced Medical Technology from The Ministry of Health, Labour and Welfare of Japan. We thank the Japan Association for the Advancement of Medical Equipment for supporting a Postdoctoral Fellowship for Dr. Jose Mario Barichello.

References

Behlke, M.A., 2006. Progress towards in vivo use of siRNAs. Mol. Ther. 13, 644–670.
Brown, P.M., Silvius, J.R., 1989. Stability and fusion of lipid vesicles containing headgroup-modified analogues of phosphatidylethanolamine. Biochim. Biophys. Acta 980, 181–190.
Elbashir, S.M., Harborth, J., Lendeckel, W., Yalcin, A., Weber, K., Tuschl, T., 2001. Duplexes of 21-nucleotide RNAs mediate RNA interference in cultured mammalian cells. Nature 411, 494–498.
Faneca, H., Simoes, S., Pedroso de Lima, M.V., 2004. Association of albumin or protamine to lipoplexes: enhancement of transfection and resistance to serum. J. Gene Med. 6, 681–692.
Godbey, W.T., Wu, K.K., Mikos, A.G., 1999. Tracking the intracellular path of poly(ethylenimine)/DNA complexes for gene delivery. Proc. Natl. Acad. Sci. U.S.A. 96, 5177–5181.
Gratton, S.E.A., Ropp, P.A., Pohlhaus, P.D., Luft, J.C., Madden, V.J., Napier, M.E., DeSimone, J.M., 2008. The effect of particle design on cellular internalization pathways. Proc. Natl. Acad. Sci. U.S.A. 105, 11613–11618.
Hoekstra, D., Rejman, J., Wasungu, L., Shi, F., Zuhorn, I., 2007. Gene delivery by cationic lipids: in and put of an endosome. Biochem. Soc. Trans. 35, 68–71.
Kaplan, I.M., Wadia, J.S., Dowdy, S.F., 2005. Cationic TAT peptide transduction domain enters cells by macropinocytosis. J Control. Release 102, 247–253.
Kawakami, S., Yamashita, F., Nishida, K., Nakamura, J., Hashida, M., 2002. Glycosilated cationic liposomes for cell-selective gene delivery. Crit. Rev. Ther. Drug Carrier Syst. 19, 171–190.
Khalil, I.A., Kogure, K., Akita, H., Harashima, H., 2006a. Uptake pathways and subsequent intracellular trafficking in nonviral gene delivery. Pharmacol. Rev. 58, 32–45.
Khalil, I.A., Kogure, K., Futaki, S., Harashima, H., 2006b. High density of octaarginine stimulates macropinocytosis leading to efficient intracellular trafficking for gene expression. J. Biol. Chem. 281, 3544–3551.
Leung, R.K.M., Whittaker, P.A., 2005. RNA interference: from gene silencing to gene-specific therapeutics. Pharmacol. Ther. 107, 222–239.
Lasic, D.D., Templeton, N.S., 1996. Liposomes in gene delivery. Adv. Drug Deliv. Rev. 20, 221–266.
Leventis, R., Silvius, J.R., 1990. Interactions of mammalian cells with lipid dispersions containing novel metabolizable cationic amphiphiles. Biochim. Biophys. Acta 1023, 124–132.
Li, C.X., Parker, A., Menocal, E., Xiang, S., Borodyansky, L., Fruehauf, J.H., 2006. Delivery of RNA interference. Cell Cycle 5, 2103–2109.
Lima, M.C.P., Simões, S., Pires, P., Faneca, H., Düzgüneş, N., 2001. Cationic lipid-DNA complexes in gene delivery: from biophysics to biological applications. Adv. Drug Deliv. Rev. 47, 277–294.
Matlin, K.S., Reggio, H., Helenius, A., Simons, K., 1982. Pathway of vesicular stomatis virus entry leading to infection. J. Mol. Biol. 156, 609–631.
Nakase, I., Niwa, M., Takeuchi, T., Sonomura, K., Kawabata, N., Koike, Y., Takehashi, M., Tanaka, S., Ueda, K., Simpson, J.C., Jones, A.T., Sugiura, Y., Futaki, S., 2004. Cellular uptake of arginine-rich peptides: roles for macropinocytosis and actin rearrangement. Mol. Ther. 10, 1011–1022.
Rejman, J., Oberle, V., Zuhorn, I.S., Hoekstra, D., 2004. Size-dependent internalization of particles via the pathways of clathrin and caveolae-mediated endocytosis. Biochem. J. 377, 159–169.
Rejman, J., Bragonzi, A., Conese, M., 2005. Role of clathrin- and caveolae-mediated endocytosis in gene transfer mediated by lipo- and polyplexes. Mol. Ther. 12, 468–474.
Sahay, G., Alakhova, D.Y., Kabanov, A.V., 2010. Endocytosis of nanomedicines. J. Control. Release 145, 182–195.
Song, E., Lee, S.-K., Dykxhoorn, D.M., Novina, C., Zhang, D., Crawford, K., Cerny, J., Sharp, P.A., Lieberman, J., Manjunath, N., et al., 2003. Sustained small interfering RNA-mediated human immunodeficiency virus type 1 inhibition in primary macrophages. J. Virol. 77, 7174–7181.
Soutschek, J., Akinc, A., Bramlage, B., Charisse, K., Constien, R., Donoghue, M., Elbashir, S., Geick, A., Hadwiger, P., Harborth, J., et al., 2004. Therapeutic silencing of an endogenous gene by systemic administration of modified siRNAs. Nature 432, 173–178.
Spagnou, S., Miller, A.D., Keller, M., 2004. Lipidic carriers of siRNA: differences in the formulation, cellular uptake, and delivery with plasmid DNA. Biochemistry 43, 13348–13356.
Thomsen, P, Roepstorff, K., Stahlhut, M., van Deurs, B., 2002. Caveolae are highly immobile plasma membrane microdomains, which are not involved in constitutive endocytic trafficking. Mol. Biol. Cell 13, 238–250.
Wadia, J.S., Stan, R.V., Dowdy, S.F., 2004. Transducible TAT-HA fusogenic peptide enhances escape of TAT-fusion proteins after lipid raft macropinocytosis. Nat. Med. 10, 310–315.
Yamakawa, S., Furuyama, Y., Oku, N., 2000. Development of a simple cell invasion assay system. Biol. Pharm. Bull. 23, 1264–1266.
Zhang, Y., Garzon-Rodriguez, W., Manning, M.C., Anchordoquy, T.J., 2003. The use of fluorescence resonance energy transfer to monitor dynamic changes of lipid-DNA interactions during lipoplex formation. Biochim. Biophys. Acta 1614, 182–192.
Zuhorn, I.S., Kalicharan, R., Hoekstra, D., 2002. Lipoplex-mediated transfection of mammalian cells occurs through the cholesterol-dependent clathrin-mediated pathway of endocytosis. J. Biol. Chem. 277, 18021–18028.

Drug Deliv. and Transl. Res. (2011) 1:277–288
DOI 10.1007/s13346-011-0025-3

RESEARCH ARTICLE

Argonaute2 is a potential target for siRNA-based cancer therapy for HT1080 human fibrosarcoma

Tatsuaki Tagami · Takuya Suzuki · Kiyomi Hirose · Jose Mario Barichello · Naoshi Yamazaki · Tomohiro Asai · Naoto Oku · Tatsuhiro Ishida · Hiroshi Kiwada

Published online: 9 April 2011
© Controlled Release Society 2011

Abstract Small interfering RNAs (siRNAs) are small RNA molecules that have a potent, sequence-specific gene silencing effect and therefore show promise for therapeutic use as molecular-targeted drugs for the treatment of various genetic diseases, including cancer. The aim of the present study was to evaluate whether Argonaute2 (Ago2) is a therapeutically effective target for siRNA-based cancer therapy. Ago2 is the key protein in mammalian RNAi and is also known as the only member of the Ago family that mediates the microRNA (miRNA)-dependent cleavage of targeted mRNAs. It is assumed that these unique properties of the Ago2 protein can play a central role in the regulation of the miRNA pathway and subsequent translational inhibition of miRNA-targeted mRNAs, including cell survival and cancer progression. To assess its therapeutic effect, siRNA against Ago2 (Ago2-siRNA) was transfected into HT1080 human fibrosarcoma cells, which are malignant cancer cells. Ago2 gene silencing resulted in the inhibition of cell growth and the induction of apoptosis and G0/G1 arrest in the cell cycle. In addition, Ago2 knockdown induced morphological changes and actin stress fiber formation in the cells. The results of a microarray study showed that Ago2 suppression stimulated several crucial genes related to apoptosis, the cell cycle, immune response, cell adhesion, metabolism, etc. Repeated intratumoral injection of Ago2-siRNA/cationic liposome complex induced tumor growth suppression in an HT1080 xenograft model. These results suggest that the suppression of the

T. Tagami · T. Suzuki · K. Hirose · J. M. Barichello · T. Ishida (✉) · H. Kiwada
Department of Pharmacokinetics and Biopharmaceutics, Subdivision of Biopharmaceutical Sciences, Institute of Health Biosciences, The University of Tokushima,
1-78-1 Sho-machi,
Tokushima 770-8505, Japan
e-mail: ishida@ph.tokushima-u.ac.jp

J. M. Barichello
Japan Association for the Advancement of Medical Equipment, Tokyo, Japan

N. Yamazaki
Department of Medicinal Biochemistry, Subdivision of Biopharmaceutical Sciences, Institute of Health Biosciences, The University of Tokushima, Tokushima, Japan

T. Asai · N. Oku
Department of Medical Biochemistry, Graduate School of Pharmaceutical Sciences, University of Shizuoka, Suruga-ku,
Shizuoka 422-8526, Japan

T. Asai · N. Oku
Global COE Program, University of Shizuoka, Suruga-ku,
Shizuoka, Japan

Present Address:
T. Tagami
Ontario Institute for Cancer Research, MaRS Centre, South Tower, 101 College Street, Suite 800,
Toronto, ON, Canada M5G 0A3

Present Address:
J. M. Barichello
Laboratory of Nanotechnology, School of Pharmacy, Universidade Federal de Ouro Preto (UFOP),
35400-000 Ouro Preto, Minas Gerais, Brazil

Ago2 gene may be useful for the inhibition of cancer progression and that Ago2 may be a desirable target for siRNA-based cancer therapy.

Keywords Argonaute2 (Ago2) · Small interfering RNA (siRNA) · RNA interference (RNAi) · Fibrosarcoma · Cationic liposome

Introduction

Fibrosarcoma is a rare malignant tumor derived from fibroblasts and is predominantly found around bone and soft tissue [1]. This tumor is associated with the abnormal disposition of collagen and other extracellular matrix components that cause invasion, after which the presence of immature blood vessels favors metastasis through the blood stream. The current treatment for inoperable fibrosarcoma is radiotherapy and chemotherapy, but the prognosis after treatment is poor [2]. A novel therapeutic modality to suppress further progression is therefore required.

RNA interference (RNAi) is a natural process that affects gene silencing in eukaryotes at the transcriptional, post-transcriptional, and/or translational levels [3]. Small interfering RNAs (siRNAs), which are short double-stranded RNA duplexes, are the key intermediates in RNAi that can potentially inhibit the expression of any targeted genes. Due to its potent, sequence-specific gene silencing effects, siRNA is a promising biological tool and potential therapeutic agent against many kinds of genetic diseases, including cancer [4]. From various points of view, many genes are seen as potential targets for siRNA-based cancer therapy. Most potential target genes for siRNA-based cancer therapy are specifically overexpressed in cancer cells, and their knockdown is less toxic to normal cells [5]. Most oncogenes have these properties, and several siRNAs against oncogenes, such as K-ras and c-myc, have shown remarkable therapeutic effects [6, 7]. Other potential target genes for siRNA therapy are those that are involved in multiple pathways or that are critical for cell survival [8]. These genes include those involved in angiogenesis (VEGF [9] and EGFR [10]), metastasis (MMPs [11]), survival (Survivin [12]), anti-apoptosis (bcl-2 [13] and XIAP [14]), resistance to chemotherapy (MDR1 [15]), and synthetic lethality (PLK1 [16] and STK33 [17]). The knockdown of these targets can effectively inhibit the many stages of cancer progression, resulting in efficient therapeutic effects. However, it is also true that familiar target genes may not be "druggable" because siRNAs against familiar genes can easily be replaced by the development of chemical inhibitors that are advantageous in molecular weight and delivery efficiency [18]. Therefore, researchers have explored the frontiers of novel target genes for siRNA-based cancer therapy.

The present study focused on the Argonaute2 (Ago2, also known as EIF2C2) gene as a novel candidate for siRNA-based cancer therapy for the following reasons: (1) Ago2 can broadly regulate both microRNAs (miRNAs) and miRNA-mediated multiple pathways, including cell survival and cancer progression. miRNAs are endogenous small RNAs that are one of the largest classes of gene regulators [19]. They regulate approximately 30% of protein-coding transcripts [20]; therefore, miRNAs control a wide range of biological processes, including cancer [21]. Some miRNAs can be oncogenic, such as the miR17-92 cluster, miR-21, etc., termed onco-miRs [22], although the function of most onco-miRs is still unclear. miRNAs are incorporated with Ago2, and then these complexes collaborate in the translational inhibition of targeted mRNAs [23]. It is therefore expected that Ago2 gene silencing can halt the development of cancer by blocking the function of miRNAs and many mRNAs regulated by miRNAs. (2) Ago2 can function as a central regulator of miRNAs. Ago2 is a member of the Ago protein family which consists of eight members in mammals [24]. Four Ago proteins are ubiquitously expressed (Ago subfamily) and the remaining four (Piwi subfamily) are expressed in germ cells. All four mammalian Ago subfamilies (Ago1 through Ago4) are associated with miRNAs, but only Ago2, which has a structure like that of RNase as a "slicer," can mediate the specific endonucleolytic cleavage of targeted mRNAs incorporated with miRNAs in mammalian cells [23, 25]. It is therefore expected that the unique and essential roles of the Ago2 gene in controlling miRNA pathways could seriously affect the survival of cancer cells. (3) As far as we know, there has been no report of severe side effects caused by inhibiting the Ago2 gene in vivo. Ago2 is a relatively well-characterized protein in the Ago family, and several reports have mentioned that Ago2 knockout is lethal to embryos because of neural tube defects [23] and defective B cell proliferation [26]. However, the shorter duration of Ago2 gene suppression induced by siRNA would not lead to such severe side effects in adult animals. For these reasons, the present study challenged Ago2 gene knockdown by transfection with siRNA against Ago2 (Ago2-siRNA) into human fibrosarcoma HT1080 cells and then characterized phenotypical changes in the cells. Global gene suppression on the mRNA level was analyzed by microarray following Ago2 gene suppression.

In addition, in this study, in vivo Ago2-siRNA delivery and antitumor effect was evaluated with a cationic liposome (TFL-3) which has been established in our previous studies [27, 28]. Cationic liposome is safer than viral vector, and its simple and easy scaling up is suitable for manufacture. Therefore, cationic liposome has been extensively investi-

gated for the delivery of nucleic acids including plasmid DNA, antisense oligonucleotide, and siRNA as translational research [13, 29–31].

Materials and methods

Cell culture

Human fibrosarcoma cells (HT1080) were obtained from Dainippon-Sumitomo Pharmaceutical (Osaka, Japan) and maintained in Dulbecco's modified Eagle's medium (DMEM, Nissui Pharmaceutical, Tokyo, Japan) supplemented with 10% heat-inactivated fetal bovine serum (FBS, Japan Bioserum, Hiroshima, Japan), 10 mM L-glutamine, 100 U/ml penicillin, and 100 μg/ml streptomycin (ICN Biomedical, OH, USA). Cells were incubated at 37°C in a humidified incubator atmosphere of 5% CO_2/95% air.

Small interfering RNAs

siRNAs were chemically synthesized and purified through HPLC by Hokkaido System Science (Hokkaido, Japan). The sequences of siRNAs were cited from previous reports as follows: siRNA for Ago2 (Ago2-siRNA), the sequence that exhibited the highest gene silencing effect in siRNAs designed in a previous report [25] (sense sequence 5′-GCA CGGAAGUCCAUCUGAAUU-3′ and antisense sequence 5′-UUCAGAUGGACUUCCGUGCUU-3′) and control siRNA (Cont-siRNA), the sequence that was targeted for firefly luciferase [32] (sense sequence 5′-CUUACGCUGA GUACUUCGATT-3′ and antisense sequence 5′-UCGAA GUACUCAGCGUAAGTT-3′).

For the preparation of siRNA duplexes, the complementary antisense and sense strands, DNase- and RNase-free grade (Nippon Gene, Tokyo, Japan), were mixed in equal amounts in TE buffer (10 μM Tris–HCl, 1 μM EDTA, pH 8.0) followed by heating at 90°C for 1 min. The reaction mixture was then allowed to cool at room temperature. The quality of siRNA duplexes was checked by 15% polyacrylamide gel electrophoresis (PAGE). The final concentration of the duplexes was 50 μM in TE buffer.

siRNA transfection

Cells were seeded at a density of 2,500 cells/well in a 96-well plate with 100 μl culture medium, 50,000 cells/well in a six-well plate with 2 ml, or 250,000 cells/well in a 10-cm dish with 10 ml as the experimental scale. At 24 h after seeding, the cells were transfected with the appropriate concentration of siRNA using LipofectAMINE 2000 (Lf 2000, Invitrogen, CA, USA) according to the manufacturer's instruction. Briefly, siRNA was premixed with Lf 2000 at a ratio of 1:5 (siRNA (micrograms)/Lf2000 (microliters)) in Opti-MEM I (Invitrogen) in a microtube, and the mixture was then held for 20 min at room temperature to form siRNA/Lf2000 complex. The siRNA/Lf2000 complex was applied to the wells or dishes, and the cells were then incubated in a medium containing FBS (final concentration 6.66% FBS). At 24 h post-transfection, the medium was replaced with fresh DMEM supplemented with 10% FBS, and the cells were then used for additional assays.

Western blotting

Western blotting was carried out as previously described [33]. Briefly, cells were seeded at a density of 250,000 cells/dish in a 10-cm dish. At 24 h after seeding, the cells were transfected with 12.5 nM of siRNA, as described above. At the indicated times after transfection (0, 24, 48, 72, and 96 h), the cells were lysed in an NP-40 lysis buffer (50 mM Tris–HCl, 1% NP-40, 0.25% sodium deoxycholate, 150 mM NaCl, pH 7.4, proteinase inhibitor cocktail; Sigma-Aldrich, MO, USA) and centrifuged at 4°C for 15 min at 15,000×*g*. The protein concentration in the supernatant was determined using a DC protein assay kit (Bio-Rad Laboratories, CA, USA). The protein extract (20 μg) was resuspended in SDS sample buffer and boiled at 95°C for 5 min, and the proteins were then separated by electrophoresis on 7% and 12% SDS-PAGE gels for Ago2 and β-actin, respectively. The proteins were transferred to PDVF Hybond-P membranes (GE Healthcare, CA, USA). Bands were blocked with Tris-buffered saline, pH 7.4, containing 3% nonfat dry milk (Beckton, Dickinson and Company, MD, USA). The membranes were incubated overnight at 4°C with primary antibodies at appropriate concentrations (1:100 for mouse monoclonal anti-Ago2 antibody (Wako, Osaka, Japan) and 1:500 for rabbit polyclonal anti-β-actin antibody (Biolegend, CA, USA)). The membranes were then further incubated with secondary antibodies conjugated with HRP-coupled anti-mouse IgG antibody (1:2,000, ICN Biomedical) or anti-rabbit antibody (1:2,000, Chemicon, CA, USA) at room temperature for 1 h. Finally, the bands were visualized by chemiluminescence using an ECL-Plus System (GE Healthcare).

RNA isolation, cDNA synthesis, and real-time PCR (quantitative RT-PCR)

RNA isolation and cDNA synthesis were performed according to the manufacturer's instructions. Briefly, cells were seeded at a density of 250,000 cells/dish in a 10-cm dish. At 24 h after the seeding, the cells were transfected with 12.5 nM of siRNA, as described above. At the

indicated times after transfection (0, 24, 48, 72, and 96 h), the total RNA of the HT1080 cells was isolated using an RNeasy Mini Kit with an RNase-Free DNase Set (Qiagen, Hilden, Germany). To conduct the reverse transcription reaction, 0.5 μg of RNA was converted to cDNA in a 1.5-ml microtube with a total volume of 20 μl, including 500 nM of Oligo(dT)$_{20}$, 500 μM dNTP, 1 μl of RNase inhibitor, and 1 μl of ReverTra Ace (Toyobo, Osaka, Japan) for 1 h at 40°C.

Real-time PCR was performed on an ABI 7000 real-time PCR system (Applied Biosystems, CA, USA) with a FastStart TaqMan Probe Master (ROX) and Universal ProbeLibrary (Roche Diagnostics GmbH, Manheim, Germany) according to the manufacturer's instructions. Briefly, the PCR mixture was applied to a 96-well plate in a total volume of 20 μl/well, including a 250 nM probe, 900 nM forward and reverse primers, 2 μl of the generated cDNA, and 10 μl of FastStart TaqMan Probe Master (ROX). The set of primers and a probe for real-time RT-PCR were designed using ProbeFinder software (Roche Diagnostics GmbH). The primers and the probes were as follows: Ago2 primers and probe (forward 5′-GTCTCTGAAGGCCAGTTCCA-3′ and reverse 5′-ATA CAGGCCTCACGGATGG-3′, probe #22) and GAPDH primers and probe (forward 5′-GCTCTCTGCTCCTC CTGTTC-3′ and reverse 5′-ACGACCAAATCCGTT GACTC-3′, probe #60). The amplification conditions were as follows: 10 min at 95°C, followed by 40 cycles of 95°C for 15 s and 60°C for 1 min. The quantity was determined from the experimental threshold cycle on a standard curve of the data from a series of serial dilutions of the mixture of generated cDNA. The Ago2 mRNA level was normalized with GAPDH as an endogenous control.

Cytotoxicity assay (MTT assay)

The cytotoxicity assay was carried out as previously described [34]. Briefly, cells were seeded at a density of 2,500 cells/well in a 96-well plate. At 24 h after seeding, the cells were transfected with various concentrations of siRNA (0, 6.25, 12.5, 25, 50, 100 nM), as described above. At the indicated times after transfection (0, 24, 48, 72, and 96 h), the cells were washed twice with PBS and 50 μl of a stock solution (5 mg/ml in PBS) of 3-(4,5-dimethylthiazol-2-yl 2,5-diphenyl) tetrazolium bromide (MTT, Nacalai Tesque, Kyoto, Japan) was added to each well. After 4 h of incubation at 37°C, the formazan crystals in the medium were dissolved in 150 μl of an acidified isopropanol solution (containing 0.04 N HCl). The formazan production was read in a plate reader using a Wallac 1420 ARVOsx multi-label counter (PerkinElmer, MA, USA) at 590 nm.

Cell apoptosis analysis

The apoptotic cells were measured using an Annexin V-FITC Apoptosis Detection Kit (Merck, Darmstadt, Germany) according to the manufacturer's instructions. Briefly, cells were seeded at a density of 50,000 cells/well in a six-well plate. At 24 h after seeding, the cells were transfected with 12.5 nM siRNA, as described above. At the indicated times after transfection (24, 48, 72, 96 h), the cells were harvested and treated with Annexin V-FITC solution for 15 min in the dark. Cell fluorescence was detected by a flow cytometer Guava EasyCyte Mini System (Guava Technologies, CA, USA), and the sample data were analyzed using CytoSoft software (Guava Technologies).

Cell cycle analysis

Cell cycle analysis was performed using a Guava cell cycle reagent kit (Guava Technologies) according to the manufacturer's instructions. Briefly, cells were seeded at a density of 50,000 cells/well in a six-well plate. At 24 h after seeding, the cells were transfected with 12.5 nM siRNA, as described above. At 48 h post-transfection, the cells were harvested, fixed with 70% ethanol, and then treated with Guava cell cycle reagent for 30 min in the dark. Cell cycle analysis for DNA content was measured using a flow cytometer (Guava Technologies). The cell cycle profile (percentage of cells within G0+G1, S, G2+M, and SubG1 phases) was analyzed using CytoSoft software (Guava Technologies).

Observation of cellular morphology and actin stress fiber by microscopy

The cell specimen for the visualization of actin fiber in cells was prepared as previously described [35]. Briefly, cells were seeded at a density of 5,000 cells/well in a 35-mm glass-based dish (Iwaki, Chiba, Japan) with 200 μl of complete culture medium. At 24 h after seeding, the cells were transfected with 12.5 nM siRNA, as described above. At 48 h post-transfection, the cells were fixed with 4% paraformaldehyde for 30 min at room temperature. Cellular morphology was observed by phase contrast microscopy (LSM510, Carl Zeiss, Oberkochen, Germany). To further visualize the actin stress fiber in the cells, they were permeated with 1% Triton X for 15 min and then stained with 0.2 μM phalloidin-FITC (Sigma-Aldrich) for 1 h at room temperature in a dark room. Actin stress fibers in cells were observed by confocal microscopy (LSM510, Carl Zeiss).

Microarray analysis

A Whole Human Genome Oligo Microarray 44Kx4pack (Agilent Technologies, CA, USA) was used as previously described [36]. Briefly, cells were seeded at a density of 250,000 cells/dish in a 10-cm dish. At 24 h after seeding, the cells were transfected with 12.5 nM of siRNA, as described above. At 48 h post-transfection, the total RNA was isolated using an RNeasy Mini Kit with an RNase-Free DNase Set (Qiagen). The quality of total RNA samples, based on the 28S/18S rRNA ratio, was assessed using an Agilent 2100 Bioanalyzer (Agilent Technologies). The RNAs were amplified, converted to the complementary DNAs, and labeled with Cy3-CTP using a Low RNA Fluorescent Agilent Linear Amplification kit (Agilent Technologies). The amplified complimentary RNA products were labeled with Cy3. The labeled cRNAs were then fragmented and hybridized using Agilent's in situ hybridization plus kit on a Human1A ver.2 Oligo Microarray (Agilent Technologies). The microarrays were scanned with an Agilent Technologies Microarray Scanner (Agilent Technologies) at 5-μm resolution. For comparative analysis between Ago2-siRNA-treated cells and Cont-siRNA-treated cells, the genes that were statistically significant using a two-sample t test ($p<0.05$, $n=3$) were identified and subsequently categorized by gene ontology. The data were analyzed using GeneSpring software (Agilent Technologies).

Antitumor efficacy of intratumor injection of siRNA/cationic liposome complex in a xenograft model

Male Balb/c Slc-nu/nu (20–25 g) mice were purchased from Japan SLC (Shizuoka, Japan). The experimental animals were allowed free access to water and chow and were housed under controlled environmental conditions (constant temperature, humidity, and 12-h dark/light cycle). All animal experiments were evaluated and approved by the Animal and Ethics Review Committee of the University of Tokushima.

To establish the tumor-bearing mouse model, 1×10^6 HT1080 cells (in 100 μl DMEM) were subcutaneously inoculated into the right flank of the mice. When the tumor was palpable (about 100 mm^3), treatment was started (day 0). For in vivo transfection of siRNA, we used TFL-3 cationic liposome, which has shown high transfection efficiency as the carrier of siRNA, as previously described [27]. TFL-3, consisting of the cationic lipid *O*,*O*′-ditetradecanoyl-*N*-(α-trimethyl ammonioacetyl) diethanolamine chloride, cholesterol, and dioleoylphosphatidylethanolamine in a molar ratio of 1.00:0.75:0.75 was generously donated by Daiichi-Sankyo Pharmaceutical (Tokyo, Japan) as a lyophilized liposome. Briefly, siRNA solution (40 μg) was directly added to the lyophilized liposomal powder (4 μmol) at a charge ratio of 7.62 (cationic lipid (+)/siRNA (−)) with vigorous vortexing (3,200 rpm, 10 min) to form the siRNA/liposome complex, which is referred to as the lipoplex. The lipoplex including either Ago2-siRNA, Cont-siRNA (40 μg siRNA/mouse/injection), or 9% sucrose solution (50 μl/injection) was directly injected into the xenografts on days 0, 2, 4, 6, 8, and 10. The antitumor effect was evaluated in terms of both tumor volume and survival. Tumor size was assessed in two dimensions and calculated by the following formula: $1/2\times\text{length}\times\text{width}^2$ [37]. Body weight was measured simultaneously and was taken as a parameter of systemic toxicity.

Statistical analysis

All values are expressed as the mean±SD. Statistical analysis was performed via a two-tailed unpaired t test and one-way ANOVA using GraphPad InStat software (GraphPad Software, CA, USA). The level of significance was set at $p<0.05$.

Results

Gene silencing effect of the transfection of Ago2-siRNA

The Ago2 gene expression in HT1080 cells was initially characterized after the transfection of Ago2-siRNA. Western blotting was performed to examine the Ago2 gene expression at the protein level (Fig. 1a). Expression of Ago2 protein was strongly suppressed in cells at 24 h after the transfection of 12.5 nM of Ago2-siRNA, but was not affected by the transfection of Cont-siRNA. This inhibitory effect of Ago2 protein continued until 96 h post-transfection. The Ago2 gene expression at the mRNA level was also examined after the transfection of Ago2-siRNA (Fig. 1b). qRT-PCR was performed in order to quantify the knock-down efficiency, and consequently, Ago2 mRNA expression was significantly inhibited to 4.4% of Cont-siRNA-treated cells at 24 h after the transfection of Ago2-siRNA. Strong inhibitory effects were observed at 48 h (5.5%) and at 72 h (11.7%) post-transfection, and subsequently, Ago2 mRNA expression was gradually increased to 20.2% even at 96 h post-transfection. Cont-siRNA-treated cells exhibited no significant change in Ago2 mRNA expression compared with untreated cells.

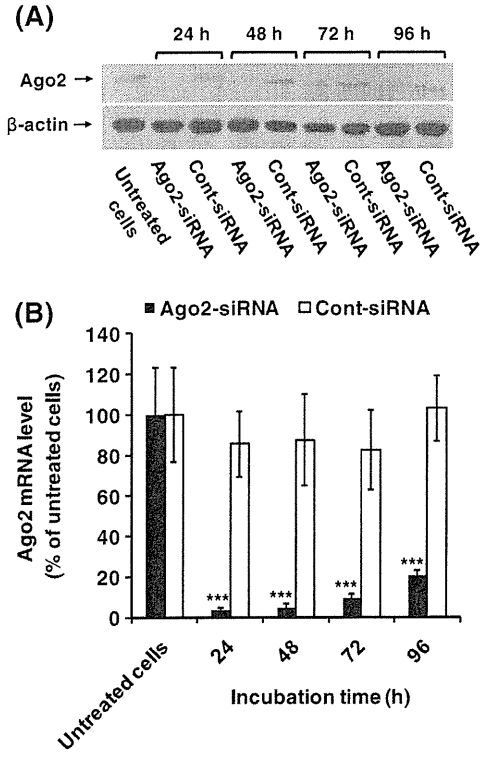

Fig. 1 Suppression of Ago2 gene expression by the transfection of Ago2-siRNA in HT1080 cells. Expressions of Ago2 protein (100 kDa) and mRNA were detected by Western blot (**a**) and qRT-PCR (**b**) analyses, respectively. Of Ago2-siRNA or Cont-siRNA, 12.5 nM was transfected into cells using Lf2000. At the indicated time post-transfection (24, 48, 72, and 96 h), total protein or RNA in the cells was extracted and analyzed as described in "Materials and methods." Data represent the mean of three separate experiments (Western blot). Each value represents the mean±S.D (n=3). ***p< 0.005 compared with Cont-siRNA-transfected cells

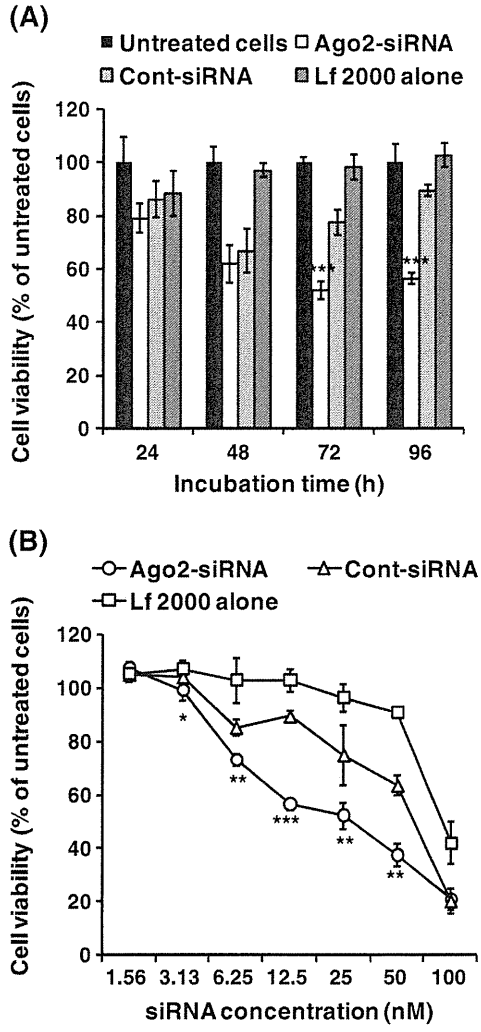

Fig. 2 Effect of Ago2 gene suppression on cell growth inhibition in HT1080 cells. **a** Time course study of cell viability. Of Ago2-siRNA or Cont-siRNA, 12.5 nM was transfected into cells using Lf2000. At the indicated times post-transfection (24, 48, 72, and 96 h), cell viability was determined by MTT assay as described in the "Materials and methods." **b** Dose dependency of cell viability. Various concentrations of siRNA (0, 6.25, 12.5, 25, 50, and 100 nM) were transfected into cells using Lf2000. At 96 h post-transfection, cell viability was determined by MTT assay as described in "Materials and methods." The amount of Lf2000 in the Lf2000 alone was set as equal to the lipoplex. Each value represents the mean±SD (n=3).*p<0.05, ***p< 0.005 compared with Cont-siRNA-transfected cells

Inhibition of growth of HT1080 cells by Ago2 gene suppression

The anti-proliferative activity of Ago2 suppression in HT1080 cells was investigated by means of an MTT assay (Fig. 2a). At 24 and 48 h post-transfection, both Ago2-siRNA and Cont-siRNA treatments indicated a similar trend in cell growth inhibition. This might be due to non-specific cytotoxicity derived from the siRNA/Lf2000 transfection reagent complex. It was previously reported that some transfection reagents, including cationic lipid-based liposome, cause cytotoxicity, and the inclusion of nucleic acids such as pDNA further increases cytotoxicity [36, 38]. Such non-selective cytotoxicity induced by transfection might mask the anti-proliferative effect selectively caused by Ago2 gene suppression. In addition, off-target effect induced by transfected siRNA could not be excluded on this non-specific cell growth inhibition. In contrast, at 72 and 96 h post-transfection, while the growth of Cont-siRNA-treated cells had restarted, the growth of Ago2-siRNA-treated cells was still attenuated. The siRNA dose dependency of cell growth was also investigated (Fig. 2b). All treatments inhibited growth in a dose-dependent manner. In particular, Ago2-siRNA treatment showed the most significant inhibitory effect in the range from 6.25 to 50 nM compared with Cont-siRNA. The most significant difference in cell growth between Ago2-siRNA and Cont-siRNA was observed at a dose of 12.5 nM of siRNA (p<0.005). The IC_{50} value of each treatment was

24.7 nM for Ago2-siRNA, 59.9 nM for Cont-siRNA, and 93.4 nM for Lf 2000 alone.

Induction of cell apoptosis by Ago2 gene suppression

The proportion of apoptosis in HT1080 cells induced by Ago2 suppression was also investigated (Fig. 3). At 24 h post-transfection, large numbers of apoptotic cells were observed in both Ago2-siRNA- and Cont-siRNA-treated cells, presumably due to transfection with the siRNA/Lf2000 transfection reagent complex. However, at 48 h after transfection, Ago2-siRNA treatment exhibited a significant apoptotic effect compared with Cont-siRNA. Extensive induction of apoptosis by Ago2 gene suppression was continuously observed up to 96 h.

Induction of G0/G1 cell cycle arrest by Ago2 gene suppression

The distribution of HT1080 cells in cell cycle stages at 48 h post-transfection was analyzed in order to evaluate intracellular events induced by Ago2 gene suppression (Fig. 4). Ago2-siRNA treatment significantly increased accumulation at the G0/G1 phase (55.2±2.1%) compared with Cont-siRNA treatment (48.0±2.65%). At the same time, the cells at the S and G2/M phases were significantly reduced (S phase, 10.2 ±0.31% by Ago2-siRNA vs. 16.0±3.0% by Cont-siRNA; G2/M phase and 18.8±1.5% by Ago2-siRNA vs. 25.3±1.3% by Cont-siRNA). The cells at the SubG1 phase, which

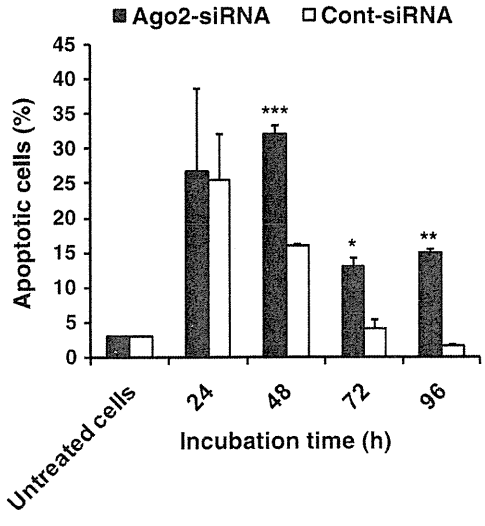

Fig. 3 Effect of Ago2 gene suppression on the induction of apoptosis in HT1080 cells. Ago2-siRNA or Cont-siRNA (12.5 nM) was transfected into cells using Lf2000. At the indicated times post-transfection (24, 48, 72, and 96 h), the proportion of apoptotic cells that were mean Annexin V-FITC positive cells was measured by flow cytometry as described in "Materials and methods." Each value represents the mean±SD (n=3).*p<0.05, ***p<0.005 compared with Cont-siRNA-transfected cells

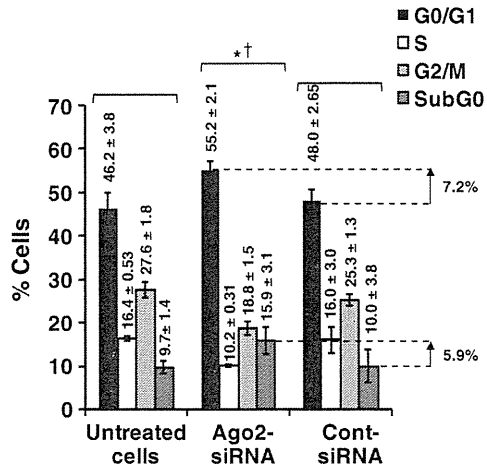

Fig. 4 Effect of Ago2 gene suppression on the distribution of cells in cell cycle stages in HT1080 cells. Ago2-siRNA or Cont-siRNA (12.5 nM) was transfected into cells using Lf2000. At 48 h post-transfection, the distribution of cell cycle stages in the cells was analyzed by flow cytometry as described in the "Materials and methods." Each value represents the mean±SD (n=3).*p<0.05 compared with Cont-siRNA transfected cells. †p<0.05 compared with untreated cells

represents apoptotic cells, were significantly increased by Ago2 gene suppression. This finding is consistent with earlier ones (Fig. 3). The difference between Ago2-siRNA treatment and Cont-siRNA treatment at G0/G1 and subG1 was 7.2% and 5.9%, respectively. This indicates that Ago2 gene suppression affects the cell cycle stages of HT1080 cells, resulting in G0/G1 arrest and apoptosis (subG1).

Morphological change in cells by Ago2 gene suppression

The morphology of HT1080 cells after Ago2 gene knockdown was observed. Ago2-siRNA-treated cells were flattened and assembled together and were distinguishable in appearance from untreated cells or Cont-siRNA-treated cells (Fig. 5a–c). To confirm the remarkable stress on cells treated with Ago2-siRNA, the actin cytoskeleton was stained. The formation of actin stress fibers was observed in Ago2-siRNA-treated cells, but not in the Cont-siRNA-treated cells or untreated cells (Fig. 5d–f). This finding indicates that Ago2 gene suppression induces strong cellular stress.

Change of the gene expression profile on cells treated with Ago2-siRNA

cDNA microarray analysis was carried out in order to investigate the change in global gene expression induced by Ago2 gene suppression. Approximately 25,000 genes were validated within the range of detection limits following Ago2-siRNA treatment and Cont-siRNA treatment. The cells treated with Ago2-siRNA (Fig. 6a) showed a remarkable gene

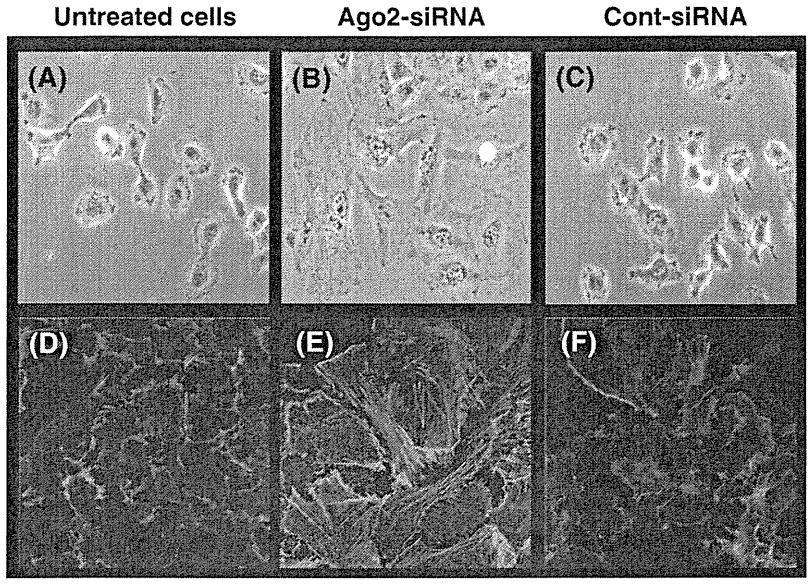

Fig. 5 Effect of Ago2 gene suppression on the cellular morphology in HT1080 cells. Ago2-siRNA or Cont-siRNA (12.5 nM) was transfected into cells using Lf2000. At 48 h post-transfection, cellular morphology was observed by phase contrast microscopy (×630 magnification, *upper panels*) (**a**–**c**). Actin organization was also visualized by staining with phalloidin-FITC, as described in "Materials and methods," and then fluorescence was observed by confocal microscopy (×630 magnification, *lower panels*) (**d**–**f**)

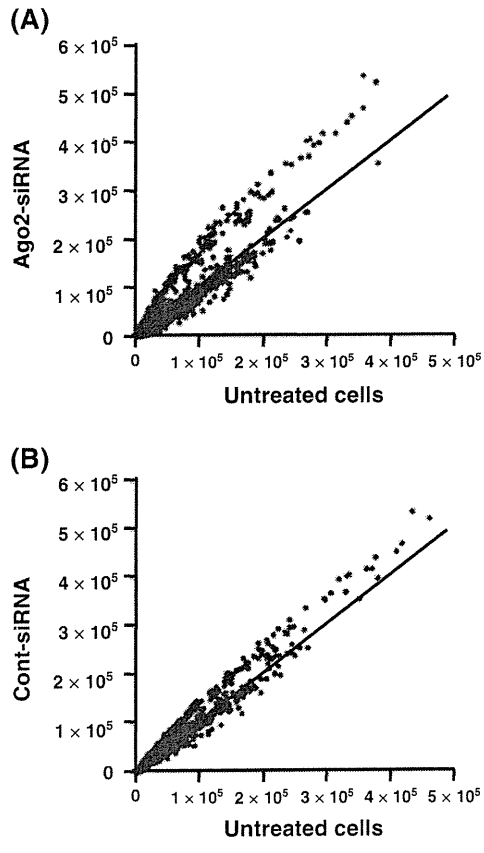

Fig. 6 Raw data scatter plot of array signals of HT1080 cells treated with Ago2-siRNA. A large number of genes (25,655) are shown. Ago2-siRNA or Cont-siRNA (12.5 nM) was transfected into cells using Lf2000. At 48 h post-transfection, total RNA was extracted and then analyzed by microarray as described in "Materials and methods." The *lines* drawn in the figure indicate the intensity ratios of genes exhibiting no changes

alteration pattern compared with the cells treated with Cont-siRNA (Fig. 6b). Filtration analysis further indicated that Ago2-siRNA treatment induced remarkable alterations in global gene expression (Table 1). The genes that were significantly up-regulated or down-regulated ($p<0.05$) in Ago2-siRNA-treated cells, as compared with those in Cont-siRNA-treated cells, were identified and categorized on the basis of gene ontology (Table 2). The genes were mostly related to apoptosis, the cell cycle, immune response, angiogenesis, cell adhesion, and metabolism.

In vivo antitumor effect of Ago2 siRNA in HT1080 xenograft model

To evaluate the in vivo therapeutic effect of Ago2 suppression, Ago2-siRNA (or Cont-siRNA)/TFL-3 cationic liposome complex (lipoplex) was injected into HT1080 tumors, which grew up under the skin. As shown in Fig. 7a,

Table 1 Up-regulated and down-regulated genes by distinct filtrations in HT1080 cells treated with Ago2-siRNA, Cont-siRNA, and Lf2000 alone

	Ago2-siRNA	Cont-siRNA
Changed >1.5-fold	3,007	1,354
Changed <1/1.5-fold	3,209	1,268
Total (%)	6,216 (24.23)	2,622 (10.22)
Changed >2-fold	998	228
Changed <1/2-fold	967	294
Total (%)	1,965 (7.66)	522 (2.03)

The total number of genes validated is 25,655

Table 2 Global change of all genes treated with Ago2-siRNA ($p<0.05$) or Cont-siRNA vs. untreated cells

GenBank	Symbol	Gene name	Fold change			p value[b]
			Ago2-siRNA[a]	Cont-siRNA[a]	(Ago2/Cont)	
Apoptosis						
NM_001003940	*BMF*	Bcl2 modifying factor isoform bmf-1	16.36	3.34	4.90	0.03
NM_000043	*FAS*	Tumor necrosis factor receptor superfamily Member 6 isoform 1 precursor	2.19	1.58	1.39	1.11E−03
NM_001429	*EP300*	E1A binding protein p300	1.51	0.99	1.53	1.82E−04
Cell cycle						
NM_000389	*CDKN1A*	Cyclin-dependent kinase inhibitor 1A	2.66	1.42	1.87	4.24E−07
AF011794	*CCPG1*	Cell cycle progression restoration 8 protein	2.06	1.62	1.27	0.01
NM_004064	*CDKN1B*	Cyclin-dependent kinase inhibitor 1B	2.02	1.00	2.02	2.18E−07
NM_005225	*E2F1*	E2F transcription factor 1	0.41	0.60	0.68	0.02
Immune response						
NM_005532	*IFI27*	Interferon, alpha-inducible protein 27	3.15	1.75	1.80	1.09E−06
NM_002982	*CCL2*	Small inducible cytokine A2 precursor	1.70	1.27	1.34	3.84E−03
NM_002502	*NFKB2*	Nuclear factor of kappa light polypeptide Gene enhancer in B cells 2 (p49/p100)	1.55	1.02	1.52	1.01E−04
NM_213662	*STAT3*	Signal transducer and activator of Transcription 3 isoform 3	1.43	1.05	1.37	1.99E−03
NM_139266	*STAT1*	Signal transducer and activator of Transcription 1 isoform beta	1.35	1.08	1.25	0.02
Angiogenesis						
NM_000029	*AGT*	Angiotensinogen preproprotein	8.10	3.82	2.12	4.06E−08
NM_003246	*THBS1*	Thrombospondin 1 precursor	2.88	0.66	4.39	4.23E−14
NM_001955	*EDN1*	Endothelin 1	2.23	1.03	2.17	1.45E−08
Cell adhesion						
NM_212482	*FN1*	Fibronectin 1 isoform 1 preproprotein	2.84	1.82	1.56	4.33E−05
NM_002210	*ITGAV*	Integrin alpha-V precursor	2.75	1.04	2.65	2.75E−10
NM_000212	*ITGB3*	Integrin beta chain, beta 3 precursor	2.38	1.60	1.48	2.19E−04
NM_004530	*MMP2*	Matrix metalloproteinase 2 preproprotein	2.20	1.06	2.08	4.11E−08
Z74615	*COL1A1*	Prepro-alpha1(I) collagen	2.16	1.01	2.15	8.14E−08
NM_133376	*ITGB1*	Integrin beta 1 isoform 1A precursor	1.42	1.18	1.20	0.049
Metabolism						
NM_002317	*LOX*	Lysyl oxidase preproprotein	1.91	1.11	1.72	3.43E−06
NM_146421	*GSTM1*	Glutathione S-transferase M1 isoform 2	1.76	1.36	1.29	9.30E−03
NM_002318	*LOXL2*	Lysyl oxidase-like 2 precursor	1.48	1.15	1.29	8.22E−03
NM_000311	*PRNP*	Prion protein preproprotein	0.14	0.99	0.14	1.01E−03
Others						
NM_000602	*SERPINE1*	Plasminogen activator inhibitor-1	3.13	2.01	1.56	4.51E−05
NM_002116	*HLA-A*	Major histocompatibility complex, class I, A precursor	1.55	1.28	1.21	0.04
NM_000021	*PSEN1*	Presenilin 1	1.43	1.09	1.31	6.03E−03

[a] Fold change compared with untreated cells

[b] Significant difference between the cells treated with Ago2-siRNA vs. Cont-siRNA

Ago2-siRNA treatment showed a remarkable tumor growth inhibition. In addition, Ago2-siRNA treatment increased the survival time of tumor-bearing mice (median survival time, 38.7 days for Cont-siRNA treatment and 28.6 days for sucrose), and as a result, more than 50% of mice (four out of seven) became long-term survivors (>70 days). Remarkable body weight loss was not observed with any treatment (data not shown).

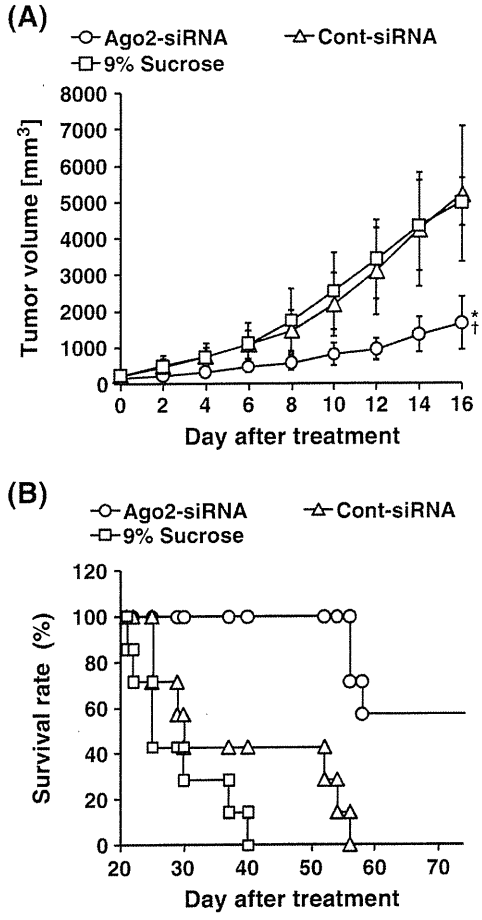

Fig. 7 Antitumor effect of Ago2-siRNA lipoplex in HT1080 xenograft model. On days 0, 2, 4, 6, 8, and 10, either Ago2-siRNA or Cont-siRNA lipoplex (40 μg siRNA per mouse per injection) or 9% sucrose solution was directly injected into the xenograft. Each treatment group included seven mice. Antitumor activity was assessed by determining the tumor size (**a**) and survival of the mice (**b**). Each value represents the mean±SD (n=7). *p<0.05 compared with treatment with Cont-siRNA lipoplex. †p<0.05 compared with treatment with 9% sucrose

Discussion

The present study showed that the suppression of the Ago2 gene significantly reduced the growth of human fibrosarcoma cells (HT1080) in vitro and in vivo, as shown in Figs. 2 and 7. This suggests that Ago2 is a desirable target for siRNA-based cancer therapy. In considering clinical application, attention should of course be paid to the influence of Ago2 gene suppression in normal tissue, which may lead to severe tissue damage. There have been very few reports that demonstrate phenotype changes after Ago2 knockout. Liu et al. [23] observed that Ago2-null mice are embryonic lethal. O'Carroll et al. [26] demonstrated that bone marrow conditional Ago2$^{-/-}$ mice have defective B cell differentiation. The duration of gene knockdown induced by siRNA is relatively shorter and more temporal than gene knockout generated genetically. The risk of damage caused by Ago2 gene suppression may be mitigated by this shorter duration in siRNA-mediated gene suppression. Such risk might also be relieved by the combination of Ago2-siRNA with a delivery system that could selectively deliver siRNA to a targeted tissue [4].

Ago2 gene suppression affected the shape of HT1080 cells. Ago2-siRNA-treated cells were flattened and thinned and gained cell–cell adhesion (Fig. 5a). The microarray study indicated enhanced expression of the genes including cell–cell adhesion in the cells (Table 2). Adam et al. [39] recently demonstrated in a breast cancer cell line that Ago2 overexpression showed a transformed phenotype, and the cells lost cell–cell adhesion as a result of down-regulation of the gene relating to cell–cell adhesion. These findings suggest that the Ago2 gene is strongly related to cell–cell adhesion in tumor cells. The loss of cell–cell adhesion and enhanced motility are known as the hallmarks of the tumorigenic progression of epithelial and endothelial cells [40]. The tumorigenic property of HT1080 cells might be relieved by treatment with siRNA against Ago2. This may result in efficient tumor growth suppression in an HT1080 xenograft model (Fig. 7). Cellular phenotypic changes induced by Ago2 gene suppression were characterized in vitro. Ago2 gene suppression exhibited an anti-proliferation effect (Fig. 2) as a result of the induction of apoptosis (Fig. 3) and G0/G1 cell cycle arrest (Fig. 4). Microarray analysis indicated a possibility that the activation of apoptosis-related genes such as Bmf and FAS is involved in the induction of apoptosis by Ago2 gene suppression (Fig. 3). Bmf (the BH3-only protein) is categorized as a pro-apoptotic member of the Bcl-2 family [41] which is involved in mitochondria-mediated apoptosis. The BH3-only protein also served as a sensor for various apoptotic stimuli, and the activation of this gene resulted in cytoskeleton damage [42]. The formation of actin stress fibers observed in Fig. 5e might result from the activation of the Bmf gene. The FAS gene is known to induce a death receptor apoptotic pathway, which is another major caspase-mediated apoptotic pathway [43]. The detection of genes involved in multiple apoptotic pathways may indicate that Ago2 gene suppression provides complex stimuli to cells. Unfortunately, overexpression of the genes that regulate the downstream apoptosis signaling pathway could not be detected under the present experimental conditions (at 48 h post-transfection). This might be due to time discrimination in the progression of the apoptosis signaling pathway. The microarray study also identified some cell cycle-related genes, CDKN1A, CCPG1, and E2F1 (Table 2). The set of CDKN1A (p21) and CDKN1B (p27) are widely known as the G1 checkpoint CDK inhibitors that regulate G1 arrest [44, 45]. E2F1 is known

as the transcriptional factor that keeps the cells in the G1 phase incorporated with Rb proteins [46]. Mack et al. [47] reported that the cell cycle of fibrosarcoma is strictly regulated by these cell cycle-related genes (CDKN1A, CCPG1, and E2F1). In addition, Abukhdeir and Park [48] reported that G0/G1 cell arrest by CDKN1A (p21) and CDKN1B (p27) is one of the major causes of the induction of cellular apoptosis in some types of cells. Therefore, following Ago2 gene suppression, HT1080 cells, halted at the G0/G1 phase, might induce apoptosis (Figs. 3 and 4). It is of interest that the *PRNP* gene was most inhibited by Ago2 gene suppression (0.14-fold, Table 2). The *PRNP* gene was originally categorized in metabolism, which is related to oxidative stress. In addition, the importance of the *PRNP* gene in cancer growth is being increasingly recognized. Studies have reported that the *PRNP* gene was overexpressed in colorectal cancer [49] and gastric cancer [50]. The overexpression of this gene accelerated cell proliferation by promoting the G1/S phase transition via the regulation of cyclin D1 [50]. These findings indicate that the down-regulation of *PRNP* by Ago2 gene suppression might attenuate the cell cycle and cell proliferation. These would be possible pathways accounting for the anti-proliferation effect mediated by Ago2 gene suppression (Fig. 2).

It is known that Ago2 broadly regulates multiple miRNAs and miRNA-mediated pathways, including cell survival and cancer progression. miRNAs, which are incorporated with Ago2, down-regulate various mRNAs [19]. Suppression of the Ago2 protein would thus lead to the accumulation of a large amount of uncleaved mRNA inside the cells and result in the breakdown of cellular function. This microarray study demonstrated that Ago2 gene suppression enhanced the global gene expressions of more than 990 genes (>2-fold changes; Fig. 6 and Table 1). The present study could not exclude the possibility that non-specific increases in the entire gene expression induce changes in cellular morphology, resulting in cellular death.

Conclusion

We found that Ago2 gene suppression mediated by Ago2-siRNA inhibited the growth of human fibrosarcoma cells in vitro and in vivo. This biological outcome was likely associated with phenotypical changes, including apoptosis, G0/G1 cell cycle accumulation, and morphological changes. The Ago2 gene, therefore, may be a desirable potential therapeutic target for siRNA-based cancer therapy.

Acknowledgments The authors thank Dr. James L. McDonald for his helpful advice in improving the manuscript. This research was supported by Research on Advanced Medical Technology in Health and Labor Science Research Grants, Ministry of Health, Labor and Welfare, Japan.

Conflict of interest Authors declare no conflict.

References

1. Taconis WK, van Rijssel TG. Fibrosarcoma of long bones. A study of the significance of areas of malignant fibrous histiocytoma. J Bone Joint Surg Br. 1985;67(1):111–6.
2. Mocellin S, Rossi CR, Brandes A, Nitti D. Adult soft tissue sarcomas: conventional therapies and molecularly targeted approaches. Cancer Treat Rev. 2006;32(1):9–27.
3. Meister G, Tuschl T. Mechanisms of gene silencing by double-stranded RNA. Nature. 2004;431(7006):343–9.
4. Akhtar S, Benter IF. Nonviral delivery of synthetic siRNAs in vivo. J Clin Invest. 2007;117(12):3623–32.
5. Huang C, Li M, Chen C, Yao Q. Small interfering RNA therapy in cancer: mechanism, potential targets, and clinical applications. Expert Opin Ther Targets. 2008;12(5):637–45.
6. Saxena N, Lahiri SS, Hambarde S, Tripathi RP. RAS: target for cancer therapy. Cancer Investig. 2008;26(9):948–55.
7. Pelengaris S, Khan M. The c-MYC oncoprotein as a treatment target in cancer and other disorders of cell growth. Expert Opin Ther Targets. 2003;7(5):623–42.
8. Aigner A. Applications of RNA interference: current state and prospects for siRNA-based strategies in vivo. Appl Microbiol Biotechnol. 2007;76(1):9–21.
9. Takei Y, Kadomatsu K, Yuzawa Y, Matsuo S, Muramatsu T. A small interfering RNA targeting vascular endothelial growth factor as cancer therapeutics. Cancer Res. 2004;64(10):3365–70.
10. Mendelsohn J, Baselga J. Epidermal growth factor receptor targeting in cancer. Semin Oncol. 2006;33(4):369–85.
11. Kargiotis O, Chetty C, Gondi CS, Tsung AJ, Dinh DH, Gujrati M, et al. Adenovirus-mediated transfer of siRNA against MMP-2 mRNA results in impaired invasion and tumor-induced angiogenesis, induces apoptosis in vitro and inhibits tumor growth in vivo in glioblastoma. Oncogene. 2008;27(35):4830–40.
12. Ryan BM, O'Donovan N, Duffy MJ. Survivin: a new target for anti-cancer therapy. Cancer Treat Rev. 2009;35(7):553–62.
13. Sonoke S, Ueda T, Fujiwara K, Sato Y, Takagaki K, Hirabayashi K, et al. Tumor regression in mice by delivery of Bcl-2 small interfering RNA with pegylated cationic liposomes. Cancer Res. 2008;68(21):8843–51.
14. Zhang Y, Wang Y, Gao W, Zhang R, Han X, Jia M, et al. Transfer of siRNA against XIAP induces apoptosis and reduces tumor cells growth potential in human breast cancer in vitro and in vivo. Breast Cancer Res Treat. 2006;96(3):267–77.
15. Stege A, Priebsch A, Nieth C, Lage H. Stable and complete overcoming of MDR1/P-glycoprotein-mediated multidrug resistance in human gastric carcinoma cells by RNA interference. Cancer Gene Ther. 2004;11(11):699–706.
16. Degenhardt Y, Lampkin T. Targeting Polo-like kinase in cancer therapy. Clin Cancer Res. 2010;16(2):384–9.
17. Scholl C, Frohling S, Dunn IF, Schinzel AC, Barbie DA, Kim SY, et al. Synthetic lethal interaction between oncogenic KRAS dependency and STK33 suppression in human cancer cells. Cell. 2009;137(5):821–34.
18. Tokatlian T, Segura T. siRNA applications in nanomedicine. Wiley Interdiscip Rev Nanomed Nanobiotechnol. 2010;2(3):305–15.
19. Sevignani C, Calin GA, Siracusa LD, Croce CM. Mammalian microRNAs: a small world for fine-tuning gene expression. Mamm Genome. 2006;17(3):189–202.
20. Bartel DP. MicroRNAs: genomics, biogenesis, mechanism, and function. Cell. 2004;116(2):281–97.

21. Nilsen TW. Mechanisms of microRNA-mediated gene regulation in animal cells. Trends Genet. 2007;23(5):243–9.
22. Cho WC. OncomiRs: the discovery and progress of microRNAs in cancers. Mol Cancer. 2007;6:60.
23. Liu J, Carmell MA, Rivas FV, Marsden CG, Thomson JM, Song JJ, et al. Argonaute2 is the catalytic engine of mammalian RNAi. Science. 2004;305(5689):1437–41.
24. Sasaki T, Shiohama A, Minoshima S, Shimizu N. Identification of eight members of the Argonaute family in the human genome small star, filled. Genomics. 2003;82(3):323–30.
25. Meister G, Landthaler M, Patkaniowska A, Dorsett Y, Teng G, Tuschl T. Human Argonaute2 mediates RNA cleavage targeted by miRNAs and siRNAs. Mol Cell. 2004;15(2):185–97.
26. O'Carroll D, Mecklenbrauker I, Das PP, Santana A, Koenig U, Enright AJ, et al. A Slicer-independent role for Argonaute 2 in hematopoiesis and the microRNA pathway. Genes Dev. 2007;21 (16):1999–2004.
27. Tagami T, Barichello JM, Kikuchi H, Ishida T, Kiwada H. The gene-silencing effect of siRNA in cationic lipoplexes is enhanced by incorporating pDNA in the complex. Int J Pharm. 2007;333(1–2):62–9.
28. Barichello JM, Ishida T, Kiwada H. Complexation of siRNA and pDNA with cationic liposomes: the important aspects in lipoplex preparation. Meth Mol Biol. 2010;605:461–72.
29. Sato Y, Murase K, Kato J, Kobune M, Sato T, Kawano Y, et al. Resolution of liver cirrhosis using vitamin A-coupled liposomes to deliver siRNA against a collagen-specific chaperone. Nat Biotechnol. 2008;26(4):431–42.
30. Gonzalez R, Hutchins L, Nemunaitis J, Atkins M, Schwarzenberger PO. Phase 2 trial of Allovectin-7 in advanced metastatic melanoma. Melanoma Res. 2006;16(6):521–6.
31. Dow S, Elmslie R, Kurzman I, MacEwen G, Pericle F, Liggitt D. Phase I study of liposome–DNA complexes encoding the interleukin-2 gene in dogs with osteosarcoma lung metastases. Hum Gene Ther. 2005;16(8):937–46.
32. Elbashir SM, Harborth J, Lendeckel W, Yalcin A, Weber K, Tuschl T. Duplexes of 21-nucleotide RNAs mediate RNA interference in cultured mammalian cells. Nature. 2001;411 (6836):494–8.
33. Asai T, Suzuki Y, Matsushita S, Yonezawa S, Yokota J, Katanasaka Y, et al. Disappearance of the angiogenic potential of endothelial cells caused by Argonaute2 knockdown. Biochem Biophys Res Commun. 2008;368(2):243–8.
34. Kobayashi T, Ishida T, Okada Y, Ise S, Harashima H, Kiwada H. Effect of transferrin receptor-targeted liposomal doxorubicin in P-glycoprotein-mediated drug resistant tumor cells. Int J Pharm. 2007;329(1–2):94–102.
35. Plattner R, Gupta S, Khosravi-Far R, Sato KY, Perucho M, Der CJ, et al. Differential contribution of the ERK and JNK mitogen-activated protein kinase cascades to Ras transformation of HT1080 fibrosarcoma and DLD-1 colon carcinoma cells. Oncogene. 1999;18(10):1807–17.
36. Tagami T, Hirose K, Barichello JM, Ishida T, Kiwada H. Global gene expression profiling in cultured cells is strongly influenced by treatment with siRNA-cationic liposome complexes. Pharm Res. 2008;25(11):2497–504.
37. Abu Lila AS, Kizuki S, Doi Y, Suzuki T, Ishida T, Kiwada H. Oxaliplatin encapsulated in PEG-coated cationic liposomes induces significant tumor growth suppression via a dual-targeting approach in a murine solid tumor model. J Control Release. 2009;137(1):8–14.
38. Nguyen LT, Atobe K, Barichello JM, Ishida T, Kiwada H. Complex formation with plasmid DNA increases the cytotoxicity of cationic liposomes. Biol Pharm Bull. 2007;30(4):751–7.
39. Adams BD, Claffey KP, White BA. Argonaute-2 expression is regulated by epidermal growth factor receptor and mitogen-activated protein kinase signaling and correlates with a transformed phenotype in breast cancer cells. Endocrinology. 2009;150 (1):14–23.
40. Fawcett J, Harris AL. Cell adhesion molecules and cancer. Curr Opin Oncol. 1992;4(1):142–8.
41. Puthalakath H, Villunger A, O'Reilly LA, Beaumont JG, Coultas L, Cheney RE, et al. Bmf: a proapoptotic BH3-only protein regulated by interaction with the myosin V actin motor complex, activated by anoikis. Science. 2001;293(5536):1829–32.
42. Jaattela M. Multiple cell death pathways as regulators of tumour initiation and progression. Oncogene. 2004;23(16):2746–56.
43. Gupta S. Molecular signaling in death receptor and mitochondrial pathways of apoptosis (review). Int J Oncol. 2003;22(1):15–20.
44. Xiong Y, Hannon GJ, Zhang H, Casso D, Kobayashi R, Beach D. p21 is a universal inhibitor of cyclin kinases. Nature. 1993;366 (6456):701–4.
45. Toyoshima H, Hunter T. p27, a novel inhibitor of G1 cyclin-Cdk protein kinase activity, is related to p21. Cell. 1994;78(1):67–74.
46. Dimova DK, Dyson NJ. The E2F transcriptional network: old acquaintances with new faces. Oncogene. 2005;24(17):2810–26.
47. Mack FA, Patel JH, Biju MP, Haase VH, Simon MC. Decreased growth of $Vhl^{-/-}$ fibrosarcomas is associated with elevated levels of cyclin kinase inhibitors p21 and p27. Mol Cell Biol. 2005;25 (11):4565–78.
48. Abukhdeir AM, Park BH. P21 and p27: roles in carcinogenesis and drug resistance. Expert Rev Mol Med. 2008;10:e19.
49. Antonacopoulou AG, Palli M, Marousi S, Dimitrakopoulos FI, Kyriakopoulou U, Tsamandas AC, et al. Prion protein expression and the M129V polymorphism of the PRNP gene in patients with colorectal cancer. Mol Carcinog. 2010;49(7):693–9.
50. Liang J, Pan Y, Zhang D, Guo C, Shi Y, Wang J, et al. Cellular prion protein promotes proliferation and G1/S transition of human gastric cancer cells SGC7901 and AGS. FASEB J. 2007;21 (9):2247–56.

© The American Society of Gene & Cell Therapy

A Double-modulation Strategy in Cancer Treatment With a Chemotherapeutic Agent and siRNA

Kazuya Nakamura[1], Amr S Abu Lila[1,2], Mariko Matsunaga[1], Yusuke Doi[1], Tatsuhiro Ishida[1] and Hiroshi Kiwada[1]

[1]Department of Pharmacokinetics and Biopharmaceutics, Institute of Health Biosciences, The University of Tokushima, Tokushima, Japan; [2]Department of Pharmaceutics and Industrial Pharmacy, Faculty of Pharmacy, Zagazig University, Zagazig, Egypt

5-Fluorouracil (5-FU) is broadly considered the drug of choice for treating human colorectal cancer (CRC). However, 5-FU resistance, mainly caused by the overexpression of antiapoptotic proteins such as Bcl-2, often leads ultimately to treatment failure. We here investigated the effect of *Bcl-2* gene silencing, using small interfering RNA (siRNA) (siBcl-2), on the efficacy of 5-FU in CRC. Transfection of siBcl-2 by a Lipofectamine2000/siRNA lipoplex effectively downregulated Bcl-2 expression in the DLD-1 cell line (a CRC), resulting in significant cell growth inhibition *in vitro* upon treatment with 5-FU. For *in vivo* treatments, S-1, an oral formulation of Tegafur (TF), a prodrug of 5-FU, was used to mimic 5-FU infusion. The combined treatment of polyethylene glycol (PEG)-coated siBcl-2-lipoplex and S-1 showed superior tumor growth suppression in a DLD-1 xenograft model, compared to each single treatment. Surprisingly, daily S-1 treatment enhanced the accumulation of PEG-coated siBcl-2-lipoplex in tumor tissue. We propose a novel double modulation strategy in cancer treatment, in which chemotherapy enhances intratumoral siRNA delivery and the delivered siRNA enhances the chemosensitivity of tumors. Combination of siRNA-containing nanocarriers with chemotherapy may compensate for the limited delivery of siRNA to tumor tissue. In addition, such modulation strategy may be considered a promising therapeutic approach to successfully managing 5-FU-resistant tumors.

Received 28 April 2011; accepted 25 July 2011; published online 30 August 2011. doi:10.1038/mt.2011.174

INTRODUCTION

Colorectal cancer (CRC) is the fourth most common malignancy worldwide, and the majority of patients is diagnosed at an advanced stage, requiring chemotherapy.[1] 5-Fluorouracil (5-FU) has been the drug of choice for the treatment of CRC for more than four decades. 5-FU is thought to exert its potent anticancer activity through its active metabolite 5-fluorodeoxyuridine diphosphate, which along with coenzyme 5,10-methylenetetrahydrofolate, forms a covalent ternary complex with thymidylate synthase, thus blocking the conversion of deoxyuridine monophosphate and, as a consequence, inhibiting DNA synthesis and inducing apoptosis.[2,3]

In recent years, a novel oral fluoropyrimidine derivative, designated S-1, has been extensively studied for its effectiveness in treating various tumors, including CRC, gastric carcinoma, pulmonary malignancy, and head and neck cancer.[4] S-1 consists of the three pharmacological agents: Tegafur (TF), 5-chloro-2,4-dihydroxypyrimidine, and potassium oxonate in a molar ratio of 1:0.4:1.[5] Its antitumor activity is achieved by the 5-FU prodrug TF. Potassium oxonate competitively inactivates gastrointestinal pyrimidine phosphoribosyl transferase, which converts 5-FU to 5-fluorouridine-5′-monophosphate, thereby reducing 5-FU-induced gastrointestinal toxicity.[6] 5-chloro-2,4-dihydroxypyrimidine competitively inhibits dihydropyrimidine dehydrogenase activity, which degrades 5-FU, resulting in an increased and prolonged retention of 5-FU in the blood.[7] S-1 has shown promising activity against CRC in clinical trials and it was found to be more effective than 5-FU. However, both 5-FU and S-1 showed a limited efficacy as a single agent for advanced CRC.[8] This limited anticancer activity was attributed mainly to the ability of tumor cells to evade apoptosis. Strategies aiming to overcome tumor cell resistance to chemotherapy via evading apoptosis are critically important.

The overexpression of the antiapoptotic protein Bcl-2, is considered one of the major mechanisms by which various cancer cells acquire resistance to apoptosis and thereby resistance to chemotherapeutic agents such as 5-FU and S-1.[9–11] Recently, several therapeutic strategies have been developed to induce silencing of the *Bcl-2* gene, thereby restoring the sensitivity of cancer cells to apoptosis-inducing cytotoxic agents. Among these strategies, RNA interference by means of small interfering RNA (siRNA) is considered an efficient approach to induce specific gene knockdown. This is achieved through specific degradation by the double-stranded siRNA of its target mRNA and has been mainly demonstrated to occur *in vitro*.[12–14] However, *in vivo* systemic delivery of siRNA to tumors has thus far remained a major challenge in gene-therapeutic anticancer strategies. Poor cellular

Correspondence: Tatsuhiro Ishida, Department of Pharmacokinetics and Biopharmaceutics, Institute of Health Biosciences, The University of Tokushima, 1-78-1 Sho-machi, Tokushima 770-8505, Japan. E-mail: ishida@ph.tokushima-u.ac.jp

uptake, short half-life, rapid systemic clearance, and the lack of selectivity for the target tissue constitute major obstacles against the efficient *in vivo* delivery of siRNA, compared to *in vitro* delivery.[15–17] Therefore, different carrier systems, based on cationic liposomes or cationic polymers, have been developed to improve/enhance *in vivo* delivery of siRNA to tumor tissues.[18–20]

The aim of this study was to investigate whether and to what extent decreased Bcl-2 protein levels, achieved by transfection of siRNA against Bcl-2 (siBcl-2), might enhance the antiproliferative and pro-apoptotic effects of 5-FU on the human CRC cell line DLD-1 *in vitro*. In addition, we evaluated the *in vivo* antitumor efficacy of a combination therapy with polyethylene glycol (PEG)-coated siBcl-2 lipoplex and S-1, in a DLD-1 xenograft mouse model.

RESULTS

Gene knockdown effect of siBcl-2 in DLD-1 cells *in vitro*

We first investigated the ability of an anti-Bcl-2 siRNA lipoplex (siBcl-2) to inhibit the expression of Bcl-2 in DLD-1 cells using western blotting. As shown in **Figure 1a,b**, siBcl-2 treatment significantly inhibited the expression of Bcl-2 up to 70%. As we observed no significant difference in gene knockdown effect between the highest two concentrations of siRNA, we used in further *in vitro* experiments at a siBcl-2 concentration of 6.25 nmol/l. The expression of β-actin, a control protein, was not affected by siBcl-2 treatments (**Figure 1a**). Transfection with a nontargeted control siRNA (siCont), at a concentration of 12.5 nmol/l, had no effect on expression levels of Bcl-2 or β-actin (**Figure 1a**). In addition, we investigated the effect of siBcl-2 transfection on the expression of the pro-apoptotic protein Bax, which promotes apoptosis. No change in expression was observed between control (siCont)-transfected DLD-1 cells and siBcl-2-transfected ones (**Figure 1c**). As a result, Bcl-2 knockdown leads to an increase of Bax/Bcl-2 ratio in the DLD-1 cells (**Figure 1b,c**).

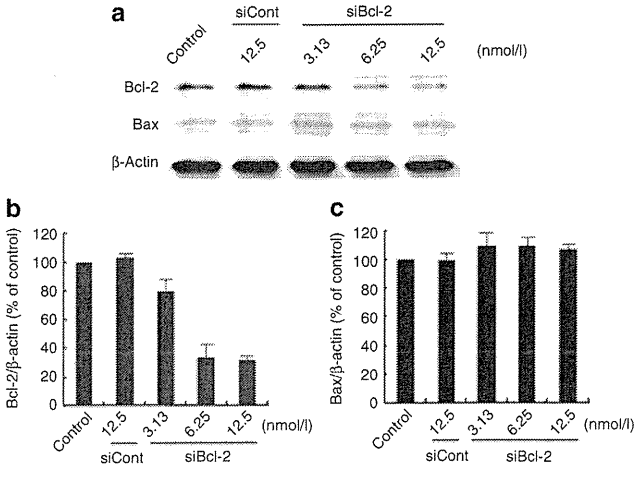

Figure 1 Examination of levels of Bcl-2 and Bax protein expression in DLD-1 cells after transfection with siRNA against Bcl-2 *in vitro*. (**a**) Western blot analysis on DLD-1 cells after transfection with siBcl-2 or siCont by Lipofectamine 2000 lipoplexes. Bands of Bcl-2 (26 kDa), Bax (20 kDa), and β-actin (42 kDa) were recorded by LAS-4000 EPUVmini. (**b**) Quantitative evaluation of the percent change in expression levels of Bcl-2 protein against β-actin one. Data represent mean ± SD from three independent experiments. (**c**) Quantitative evaluation of the percent change in levels of Bax protein against β-actin one. Data represent mean ± SD from three independent experiments. siRNA, small interfering RNA.

Cytotoxicity and induction of apoptosis by the combined treatment of DLD-1 cells with siRNA and 5-FU

It has been reported that high expression of Bcl-2 protein is associated with increased resistance of cancer cells to chemotherapeutic agents such as 5-FU via protecting the cells against induction of apoptosis.[21,22] Therefore, we investigated whether siBcl-2-induced Bcl-2 knockdown enhances the antiproliferative effect of 5-FU on DLD-1 cells. As shown in **Figure 2a**, 5-FU treatment decreased cell viability in a dose-dependent manner with an IC_{50} (drug concentration inducing 50% growth inhibition) of 0.48 μg/ml. The transfection of siBcl-2 shifted the IC_{50} of 5-FU from 0.48 μg/ml to 0.20 μg/ml, while transfection with siCont caused no change in IC_{50}. Apparently, siBcl-2-transfected DLD-1 cells became more chemosensitive to 5-FU.

In order to investigate the antiproliferative effect of siBcl-2, apoptosis was determined using TdT-mediated dUTP Nick-End Labeling (TUNEL) staining following either one single treatment (5-FU or siBcl-2) or combined treatment. As shown in **Figure 2b**, siBcl-2 transfection induced apoptosis in 15.8% of the DLD-1 cells as compared to only 4.2% in siCont-transfected cells. Monotherapy

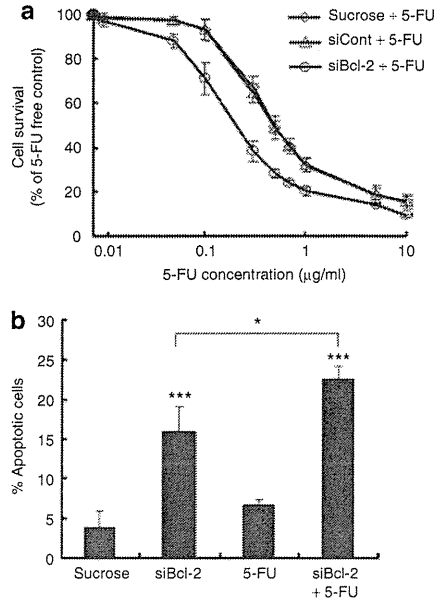

Figure 2 Effect of the combined treatment of siBcl2 and 5-FU on viability and apoptosis of DLD-1 cells *in vitro*. (**a**) Effect of different concentrations of 5-FU on cell viability of nontreated, siCont-treated, and siBcl-2-treated DLD-1 cells. Cell viability was determined by MTT assay. (**b**) Effect of single or combined treatment with siBcl-2 (6.25 nmol/l) and 5-FU (0.5 μg/ml) on apoptosis in DLD-1 cells. Apoptotic cells were detected by TUNEL assay. Data were represented from three independent experiments. ***$P < 0.001$ versus nontreated cells (none). *$P < 0.05$ siBcl-2 and siBcl-2 + 5-FU. 5-FU, 5-Fluorouracil; MTT, 3-(4,5-dimethylthiazol-2-yl)-2,5-diphenyltetrazolium bromide.

© The American Society of Gene & Cell Therapy

with 5-FU did not induce significant apoptosis at the low concentration applied (0.5 μg/ml). On the other hand, the combined treatment (siBcl-2 + 5-FU) caused a substantial induction of apoptosis (22.5% of cells). These results suggest that downregulation of Bcl-2 by siBcl-2 treatment increase cellular sensitivity to 5-FU as a result of promoting induction of apoptosis.

In vivo tumor growth suppression by the combined treatment with siBcl-2 and S-1

In order to apply the *in vitro* findings to the *in vivo* situation, we investigated the antitumor effect of combined treatment of PEG-coated siBcl-2-lipoplexes and S-1 in a DLD-1 xenograft mouse model (**Figure 3**). Treatment with siCont-lipoplexes did not result in any suppressive effect on tumor growth. Single treatment with either siBcl-2-lipoplex or S-1 resulted in a moderate inhibition of tumor growth. The combined treatment of siBcl-2-lipoplexes with S-1, however, induced remarkable tumor growth suppression. In addition, monotreatment with siBcl-2-lipoplex or S-1 resulted in15% and 28% reduction in tumor weight respectively, whereas treatment with the combination of siBcl-2-lipoplex with S-1 resulted in a tumor weight reduction of as much as 62% (**Figure 3b**). Moreover, through all therapeutic treatments, no significant body weight loss upon treatment was observed (**Supplementary Figure S1**). These results indicate that combined treatment with siBcl-2-lipoplex and S-1 produces synergistic tumor growth suppression without causing severe toxicity in a human CRC xenograft mouse model.

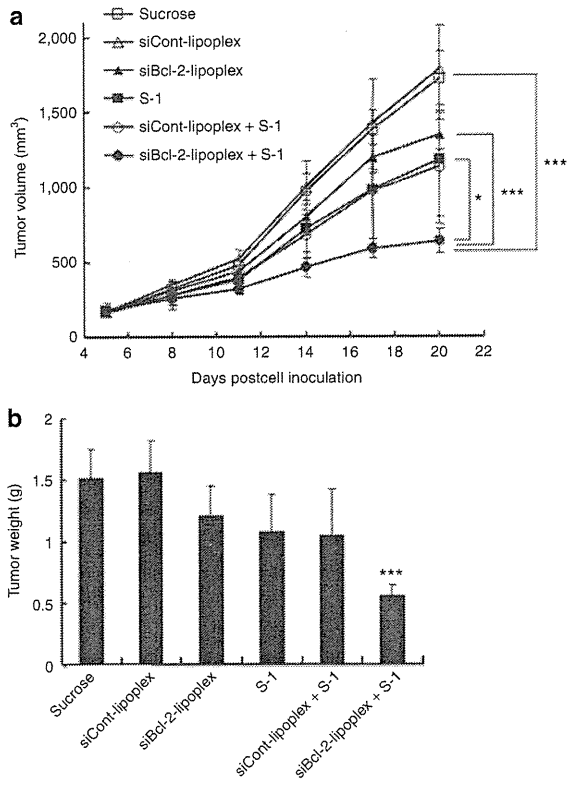

Figure 3 Tumor growth suppressive effect of the combined treatment of PEG-coated siBcl-2-lipoplexes and S-1 in the DLD-1 bearing mouse model. (**a**) Tumor volume following treatments. Tumor xenografts were established by subcutaneous implantation of DLD-1 cells in nude mice. S-1 (6.9 mg/kg) was orally administered daily from day 5 to 19 after tumor cell inoculation. PEG-coated siRNA-lipoplexes containing either siCont or siBcl2 (10 μg siRNA/mouse) were intravenously administered every 2 days (on day 5, 7, 9, 11, 13, 15, 17, and 19 after tumor cell inoculation). For the control group, sucrose was administered instead of S-1 and PEG-coated siRNA lipoplexes. (**b**) Tumor weight on day 21 post-tumor inoculation. Data represent mean ± SD ($n = 6$). ***$P < 0.001$ versus control. PEG, polyethylene glycol.

In vivo Bcl-2 knockdown and apoptosis induction in tumor tissue following combined treatment with siBcl-2 and S-1

The Bcl-2 and Bax protein levels in the treated tumor were determined by western blot analysis (**Figure 4a**). Treatment with siBcl-2-lipoplex did not induce downregulation of Bcl-2 protein, whereas S-1 treatment slightly suppressed Bcl-2 protein expression. The combined treatment with siBcl-2-lipoplex and 5-FU

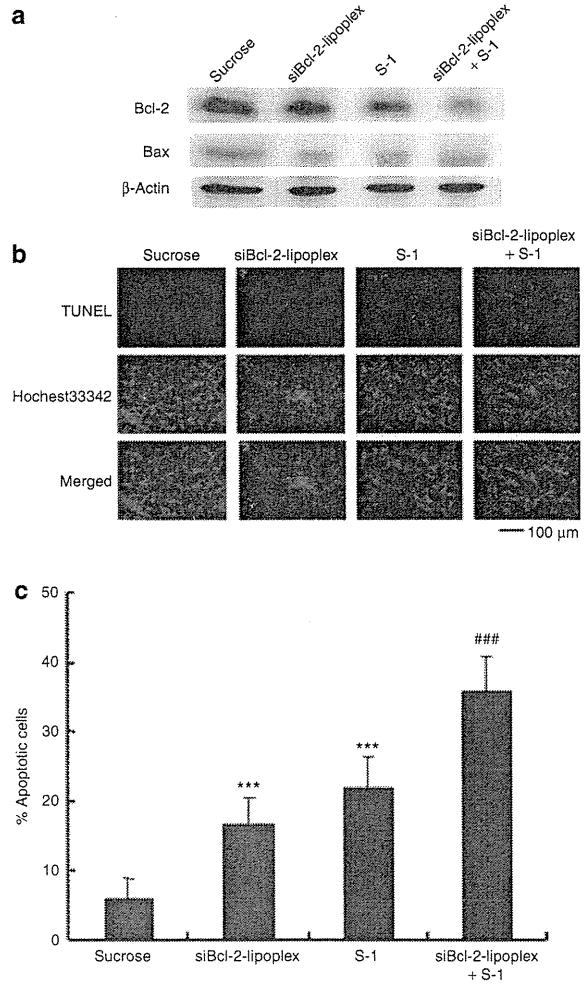

Figure 4 Suppression of Bcl-2 protein expression and induction of apoptosis in the tumor tissue after *in vivo* treatment. (**a**) Bcl-2 and Bax protein expression was determined by western blot analysis. β-actin protein was used for equal loading assessment. (**b**) Numbers of apoptotic cells in the tumor section were determined by TUNEL staining. (**c**) Percent of TUNEL-positive cells in the section. Data represent mean ± SD. ***$P < 0.001$ versus sucrose. ###$P < 0.001$ versus S-1 or siBcl-2-lipoplex.

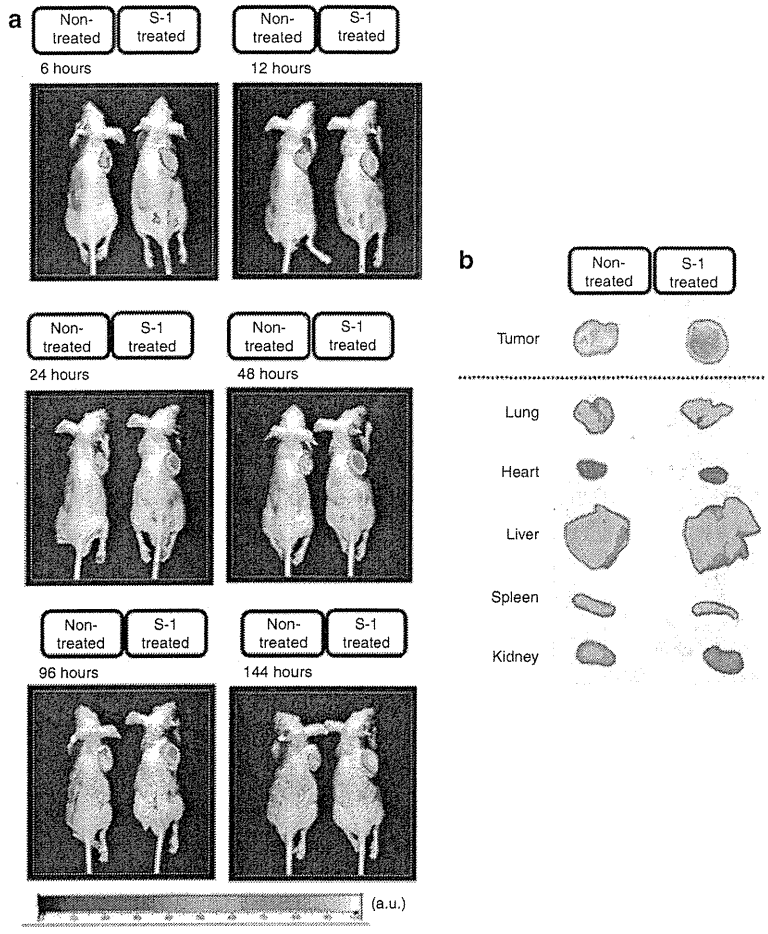

Figure 5 Effect of S-1 treatment on *in vivo* tumor accumulation of PEG-coated siRNA-lipoplexes. DLD-1 bearing mice were pretreated with or without daily S-1 dosing (6.9 mg tegafur/kg) for 7 days. On the last day of S-1 treatment, mice received an intravenous injection of DiD labeled-PEG-coated siRNA-lipoplexes. One representative picture of three independent experiments was shown here. (**a**) *In vivo* imaging of the lipoplexes at 6, 12, 24, 48, 96, and 144 hours postinjection. (**b**) Organ distribution of the lipoplexes 24 hours postinjection. PEG, polyethylene glycol.

induced remarkable downregulation of Bcl-2 protein expression. In addition, in none of the treatment groups, any change in the level of Bax expression was observed. This suggests that the combined treatment leads to an increase in Bax/Bcl-2 ratio in the tumor tissue, thus clearly rendering the intratumoral condition pro-apoptotic *in vivo*.

The apoptotic cells in the treated tumors were identified by TUNEL assay (**Figure 4b**). Combination treatment with siBcl-2-lipoplex and S-1 significantly enhanced apoptosis (apoptotic index 32.8 ± 2.4%), compared to treatment with siBcl-2-lipoplex or S-1 alone (apoptotic index 13.2 ± 1.9% and 21.2 ± 2.1%, respectively). These results emphasize that the tumor growth suppression caused by the combined treatment (**Figure 3a**) strongly relates to induction of cellular death via apoptotis in the tumor tissue (**Figure 4c**).

Effect of S-1 dosing on the intratumoral accumulation of PEG-coated siRNA-lipoplex in the DLD-1 xenograft model

The effect of daily S-1 dosing on the accumulation and biodistribution of PEG-coated siRNA-lipoplexes in the DLD-1 xenograft model was investigated semi-quantitatively by injecting DiD-labeled PEG-coated siRNA-lipoplexes intravenously into DLD-1 bearing mice pretreated with daily oral administration of either saline (control) or S-1 (6.9 mg tegafur/kg) for 7 days. Daily S-1 dosing significantly enhanced accumulation of the PEG-coated siRNA-lipoplexes in DLD-1 tumors (**Figure 5a**) at all investigated postinjection times. To assess organ distribution at 24 hours after injection, tumor, lungs, heart, liver, spleen, and kidney were collected and separately imaged (**Figure 5b**). Daily S-1 dosing enhanced accumulation of the test-lipoplexes in the tumor, but not in any of the other major organs. For a quantitative evaluation of organ distribution, mice were intravenously injected with ^{3}H-CHE-labeled PEG-coated siRNA-lipoplexes with or without prior treatment with S-1 (for 7 days). Similar to the result of the *in vivo* imaging study, daily S-1 dosing significantly enhanced the accumulation of the test PEG-coated siRNA-lipoplexes in the tumor (1.55-fold at 24 hours after injection) (**Figure 6a**), but not in lung, liver, spleen, and kidney (**Figure 6b**). These observations clearly indicate that daily S-1 dosing significantly enhances the intratumoral accumulation of PEG-coated siRNA-lipoplexes *in vivo* without affecting the distribution pattern in other major organs.

© The American Society of Gene & Cell Therapy

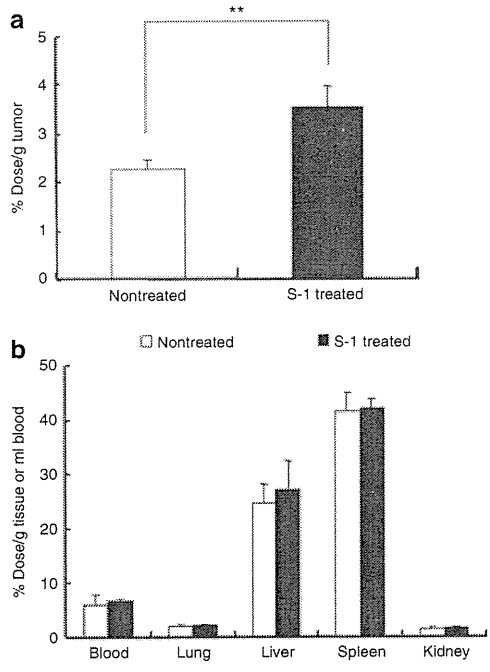

Figure 6 Effect of S-1 treatment on *in vivo* tumor accumulation and biodistribution of radio-labeled PEG-coated siRNA-lipoplexes. DLD-1 bearing mice were pretreated with or without daily S-1 dosing (6.9 mg tegafur/kg) for 7 days. On the last day of S-1 treatment, mice received an intravenous injection of ^{3}H-CHE-labeled PEG-coated siRNA-lipoplex. At 24 hours after injection, samples were collected and the radioactivity in blood and major organs was determined. (**a**) Radioactivity (%dose) in tumor tissues. (**b**) Radioactivity (%dose) in blood, lung, liver, spleen, and kidney. Data represent mean ± SD (n = 3–4). $^{**}P < 0.01$ versus control. PEG, polyethylene glycol.

DISCUSSION

The occurrence of drug resistance is a main obstacle to the success of cancer chemotherapy.[23] siRNA has been proposed as a promising novel approach to circumvent drug resistance via suppressing the expression of vital proteins involved in drug resistance mechanisms (such as MDR protein, Bcl-2, and P-glycoprotein).[14,24,25] 5-FU is a wellknown apoptosis-inducing drug and has been used in clinical settings for several decades. However, its clinical efficiency is potentially restricted by the development of drug resistance.[26,27] Among the various reported mechanisms of resistance to 5-FU, we aimed in the present study at a cell signaling protein, Bcl-2 protein. It was assumed that the downregulation of Bcl-2 protein by siRNA transfection may be a useful strategy to restore the chemosensitivity of 5-FU against many resistant cancer cell lines. Therefore we evaluated the effect of siRNA against Bcl-2 (siBcl-2) on the expression of Bcl-2 and the chemosensitivity against 5-FU in DLD-1 cells, a colon cancer cell line. Anti-Bcl-2 siRNA complexed to Lipofectamine 2000 (siBcl-2) significantly inhibited expression of Bcl-2 (**Figure 1a,b**) and increased chemosensitivity of DLD-1 cells towards 5-FU (**Figure 2a,b**).

Although several reports have mentioned the efficacy of siRNAs in silencing gene expression *in vitro*[12,13,28], poor cellular uptake, low stability, and rapid clearance of siRNA from the systemic circulation constitute major hurdles in achieving efficient systemic delivery of siRNA, which limits its efficiency *in vivo* and in clinical settings.[16,17] To achieve prolonged circulation time and enhanced cellular uptake of the siRNA, we employed PEG-coated cationic liposomes and we used S-1 instead of 5-FU. TF in S-1 is a prodrug of 5-FU and is converted into 5-FU by cytochrome p-450 which is mainly expressed in the liver.[29] The combined approach of siBcl-2-lipoplexes and S-1 showed superior tumor inhibition compared with monotherapy with either agent alone (**Figure 3a,b**). This enhanced antitumor effect of the combined approach reflects our *in vitro* results.

To elucidate the reason for enhanced antitumor activity of this combined therapy, we investigated the effect of S-1 dosing on the intratumoral accumulation of the siBcl-2-lipoplexes. **Figures 5** and **6** demonstrate that daily S-1 dosing significantly enhances the intratumoral accumulation of PEG-coated siRNA-lipoplexes. In a previous study, we showed that daily S-1 dosing enhances the intratumoral accumulation of PEG-coated neutral liposomes.[30] These results obviously demonstrate that the combined therapy of S-1 and siBcl-2 exerts its efficient antitumor activity via a double-modulation machinery; while on the one hand S-1 treatment significantly enhances the accumulation and permits efficient delivery of siBcl-2 lipoplexes into tumor tissue, at the same time the tumor-accumulated siBcl-2 lipoplexes activate the cellular apoptotic pathway, thus enhancing the cytotoxic activity of 5-FU.

Although the combination of chemotherapy and siRNA-based therapy for cancer treatment has gained increasing attention, the design of an ideal delivery strategy that can maximize the efficiency of siRNA is still a formidable challenge.[31] Many studies have emphasized the potential of a combined therapy of chemotherapeutic agents and siRNA-based therapy *in vitro*; however, *in vivo* antitumor efficiency of such combination strategy is still disappointingly low.[24,32,33] This inefficient *in vivo* activity has been attributed either to the failure to achieve efficient delivery of siRNA to tumor tissue or to the inefficient gene knockdown effect caused by the delivered siRNA.[34,35] In this study, however, we succeeded to develop a PEG-coated siRNA-lipoplex and we found that S-1 administered simultaneously with siBcl-2-lipoplexes exerted an enhancing effect on the intratumoral accumulation of siBcl-2-lipoplexes allowing preferential accumulation of siRNA-lipoplexes in the tumor. This enhanced accumulation of siRNA-lipoplexes, together with S-1 administration, permitted a synergistic tumor suppression effect *in vivo* following systemic administration of the combination therapy. In this study, we showed that combined therapy of S-1 and siRNA targeted against the antiapoptotic protein Bcl-2 has a potent tumor-suppressive activity via a double-modulation machinery: S-1 chemotherapy permits preferential accumulation of siRNA lipoplexes in tumor tissue whereas the accumulated siRNA sensitizes tumor cells to the action of the chemotherapy. This double-modulation approach offers a novel therapeutic strategy of high potential for controlling the aggressive growth of human CRCs.

MATERIALS AND METHODS

Materials. 5-FU and S-1 were generously donated by Taiho Pharmaceutical (Tokyo, Japan). 1-palmitoyl 2-oleoyl phosphatidylcholine (POPC), dioleoylphosphatidylethanolamine (DOPE), and 1,2-distearoyl-sn-glycero-3-phosphoethanolamine-n-(methoxy (polyethyleneglycol)-2000) ($mPEG_{2000}$-DSPE) were generously donated by NOF (Tokyo, Japan).

Cholesterol (CHOL), hyaluronic acid sodium salt from rooster comb (HA), and protamine sulfate from salmon (PRO) were purchased from Wako Pure Chemical (Osaka, Japan). O,O′-ditetradecanoyl-N-(alpha-trimethyl ammonio acetyl) diethanolamine chloride (DC-6-14) as a cationic lipid was purchased from Sogo Pharmaceutical (Tokyo, Japan). 1,1′-dioctadecyl-3,3,3′,3′-tetramethylindodicarbocyanine perchlorate (DiD), Opti-MEM I, and Lipofectamine 2000 were purchased from Invitrogen (San Diego, CA). ^{3}H-cholesterylhexadecyl ether (^{3}H-CHE) was purchased from PerkinElmer Japan (Yokohama, Japan). All other reagents were of analytical grade.

Animals and tumor cell line. 5-week-old male BALB/c *nu/nu* mice were purchased from Japan SLC (Shizuoka, Japan). The experimental animals were allowed free access to water and mouse chow, and were housed under controlled environmental conditions (constant temperature, humidity, and 12-hour dark–light cycle). All animal experiments were evaluated and approved by the Animal and Ethics Review Committee of the University of Tokushima. A human colon carcinoma cell line, DLD-1, was kindly provided by Taiho Pharmaceutical and was maintained in RPMI-1640 medium (Wako Pure Chemical) supplemented with 10% heat-inactivated fetal bovine serum (Japan Bioserum, Hiroshima, Japan), 100 units/ml penicillin, and 100 μg/ml streptomycin (ICN Biomedicals, Irvine, CA) in a 5% CO_2/air incubator at 37 °C.

siRNAs. All siRNAs, chemically synthesized and purified by high-performance liquid chromatography, were purchased from Nippon EGT (Toyama, Japan). The sequence of siRNA against Bcl-2 (siBcl-2) was sense: 5′-UGU GGA UGA CUG AGU ACC UGA-3′ and antisense: 5′-UCA GGU ACU CAG UCA UCC ACA GG-3′.[36] siRNAs against firefly luciferase was used as a negative control (siCont). The sequence against luciferase was sense: 5′-CUU ACG CUG AGU ACU UCG ATT-3′ and antisense: 5′-UCG AAG UAC UCA GCG UAA GTT-3.[37] siRNAs were dissolved in RNase free water at a final concentration of 50 nmol/l.

In vitro gene knockdown by siRNA transfection. DLD-1 cells were seeded in six-well plates at a density of 3.2 × 10^4 cells/well 24 hours before siRNA transfection. The cells were transfected with 3.13, 6.25, or 12.5 nmol/l siBcl-2 or 12.5 nmol/l siCont in Opti-MEM I using Lipofectamine 2000 according to the manufacturer's recommended protocol. Seventy-two hours later, gene silencing was examined with western blotting as described below.

Treated cells were washed with chilled phosphate buffered saline (37 mmol/l NaCl, 2.7 mmol/l KCl, 8.1 mmol/l Na_2HPO_4, and 1.47 mmol/l KH_2PO_4; pH 7.4) and were lysed in ice-cold lysis buffer containing 50 mmol/l Tris-HCl (pH 7.4), 1% NP-40, 0.25% sodium deoxycholate, 150 mmol/l NaCl, and protease inhibitor cocktail (Sigma-Aldrich, St Louis, MO). The lysate was collected into a 1.5 ml Eppendorf tube and then centrifuged at 4 °C for 15 minutes at 15,000*g*. The protein concentrations in lysates were determined with the Bio-Rad DC Protein Assay kit (Bio-Rad Laboratories, Hercules, CA) with bovine serum albumin (Sigma-Aldrich) as a standard according to the manufacturer's recommended instruction. Equivalent amounts of protein (40 μg) from each cell lysate were separated on a 15% SDS-PAGE gel and transferred electrophoretically onto Hybond-ECL (GE Healthcare, Cleveland, OH). The membranes were blocked with Tris-buffered saline containing 0.05% Tween 20 and 3% nonfat dry milk powder for 1 hour at room temperature and then incubated overnight at 4 °C with primary antibodies: mouse monoclonal anti-human Bcl-2 antibody (BD Biosciences, San Jose, CA), mouse monoclonal anti-human Bax antibody (BD Biosciences), and mouse monoclonal anti-human β-actin antibody (BioVision, Mountain View, CA), respectively. β-actin was used as a loading control. After three washes with Tris-buffered saline containing 0.05% Tween 20, membranes were incubated with horseradish peroxidase-conjugated goat anti-mouse secondary antibody (MP Biomedicals, Solon, OH) for 1 hour at room temperature. After an additional three washes with Tris-buffered saline containing 0.05% Tween 20, membranes were processed for enhanced chemiluminescence using the ECL Plus Chemiluminescence Reagent (GE Healthcare UK, Little Chalfont, UK), and the obtained images were analyzed using LAS-4000 EPUVmini and Multi Gauge v.3.2 (FujiFilm, Tokyo, Japan).

In vitro cellular chemosensitivity to 5-FU. Cellular chemosensitivity to 5-FU was detected by the 3-(4,5-dimethylthiazol-2-yl)-2,5-diphenyltetrazolium bromide (MTT) assay and by the TUNEL apoptosis assay using In Situ Cell Death Detection Kit, TMR Red (Roche Diagnostics, Mannheim, Germany).

To determine the cytotoxicity of single-drug treatment and combined treatment of siBcl-2 and 5-FU, DLD-1 cells were seeded in 96-well plates at a density of 2 × 10^3 cells/well 24 hours before siRNA transfection. The cells were transfected with 6.25 nmol/l siBcl-2 or siCont for 24 hours as described above. After transfection, the culture medium was replaced with fresh medium containing various concentrations of 5-FU ranging from 0.01 to 10 μg/ml. Following 96 hours incubation at 37 °C, the cells were further incubated with 50 μl MTT reagent (5 mg/ml; MP Biomedicals) for 4 hours at 37 °C. Then, 150 μl of acid-isopropanol (0.04 N HCl in isopropanol) was added to each well to dissolve formazan crystals. The absorbance of each well was read at 570 nm on a microplate reader, Wallac1420 ARVOsx (PerkinElmer Life Sciences, Boston, MA). The cell survival value index was calculated as $(A_{570\ (5\text{-}FU(+))}/A_{570\ (5\text{-}FU(-))}) \times 100$ (%). Data shown are representative of three independent experiments.

For detection of apoptosis after treatments, the cells were seeded in six-well plates at a density of 4 × 10^4 cells/well 24 hours before siRNA transfection. The cells were transfected with 6.25 nmol/l of either siBcl-2 or siCont by Lipofectamine 2000 for 24 hours as described above. After transfection, the culture medium was replaced with fresh medium with or without 5-FU (0.5 μg/ml). Following a 96-hour incubation at 37 °C, the apoptotic cells in the treated wells were determined according to the manufacturer's recommended protocol.

Preparation of PEG-coated siRNA-lipoplexes

Cationic liposomes. Cationic liposomes, composed of DOPE:POPC: CHOL:DC-6-14 (3:2:3:2, molar ratio), were prepared as previously described.[38] Briefly, the lipids were dissolved in chloroform and after evaporation of the organic solvent, the resulting lipid film was hydrated in 9% sucrose to produce multilamellar vesicles. The multilamellar vesicles were sized by repeated extrusion through polycarbonate membrane filters (Nuclepore, Pleasanton, CA) with consecutive pore sizes of 400, 200, 100, and 80 nm. The mean diameters and ζ-potentials of the resulting liposomes were determined using a NICOMP 370 HPL submicron particle analyzer (Particle Sizing System, Goleta, CA). The mean diameter and ζ-potential for cationic liposomes were 102.4 ± 7.6 nm and 19.8 ± 0.5 mV (n = 3), respectively. The concentration of phospholipids was determined by colorimetric assay.[39]

PEG-coated siRNA lipoplexes. PEG-coated siRNA-lipoplexes were prepared according to the method reported before[40,41] with minor modification. Briefly, to prepare Core-siRNA complexes, siRNA, HA, and PRO were mixed at a ratio of siRNA/HA/PRO = 0.9/0.9/1 (weight ratio) and incubated for 5 minutes at room temperature. For formulation of siRNA-lipoplexes, cationic liposomes, preformed as described above, and Core-siRNA complexes were mixed at a ratio of cationic liposome/siRNA = 2,000/1 (molar ratio), vortexed for 15 seconds, and then allowed to stand at room temperature for 10 minutes. For *in vivo* application, the siRNA-lipoplexes were surface-modified by PEG-conjugated lipid (PEGylation) using a postinsertion method.[42] Briefly, $mPEG_{2000}$-DSPE (5 mol% of liposomal phospholipids) in 9% sucrose solution and the prepared siRNA-lipoplexes were mixed. The mixture was vortexed for 1 minute and gently shaken for 1 hour at 37 °C. The mean diameter and ζ-potential of resulting PEG-coated siRNA-lipoplexes were 191.2 ± 47.1 nm and 18.2 ± 0.9 mV (n = 3), respectively. To check the presence of free siRNA in the prepared